nature microbiology

LETTERS

https://doi.org/10.1038/s41564-019-0619-y

# Successive blood meals enhance virus dissemination within mosquitoes and increase transmission potential

Philip M. Armstrong[1,2*], Hanna Y. Ehrlich[2], Tereza Magalhaes[3], Megan R. Miller[3], Patrick J. Conway[1,4], Angela Bransfield[1], Michael J. Misencik[1], Andrea Gloria-Soria[1], Joshua L. Warren[5], Theodore G. Andreadis[1,2], John J. Shepard[1], Brian D. Foy[3], Virginia E. Pitzer[2] and Doug E. Brackney[1,2*]

**The recent Zika virus (ZIKV) and chikungunya virus epidemics highlight the explosive nature of arthropod-borne viruses (arboviruses) transmitted by *Aedes* spp. mosquitoes[1,2]. Vector competence and the extrinsic incubation period (EIP) are two key entomological parameters used to assess the public health risk posed by arboviruses[3]. These are typically measured empirically by offering mosquitoes an infectious blood meal and temporally sampling mosquitoes to determine the infection and transmission status. This approach has been used for the better part of a century; however, it does not accurately capture the biology and behaviour of many mosquito vectors that refeed frequently (every 2–3 d)[4]. Here, we demonstrate that acquisition of a second non-infectious blood meal significantly shortens the EIP of ZIKV-infected *Aedes aegypti* by enhancing virus dissemination from the mosquito midgut. Similarly, a second blood meal increases the competence of this species for dengue virus and chikungunya virus as well as *Aedes albopictus* for ZIKV, suggesting that this phenomenon may be common among other virus–vector pairings and that *A. albopictus* might be a more important vector than once thought. Blood-meal-induced microperforations in the virus-impenetrable basal lamina that surrounds the midgut provide a mechanism for enhanced virus escape. Modelling of these findings reveals that a shortened EIP would result in a significant increase in the basic reproductive number, $R_0$, estimated from experimental data. This helps to explain how *A. aegypti* can sustain explosive epidemics such as ZIKV despite relatively poor vector competence in single-feed laboratory trials. Together, these data demonstrate a direct and unrecognized link between mosquito feeding behaviour, EIP and vector competence.**

Arthropod-borne viruses (arboviruses) represent an ongoing threat to human health as shown by the emergence and global spread of dengue virus (DENV; Flaviviridae), chikungunya virus (CHIKV; Togaviridae) and ZIKV (Flaviviridae)[5,6]. These three arboviruses are transmitted by mosquitoes of the genus *Aedes*, subgenus *Stegomyia*, which serve as epidemic vectors, and are known to cause disease outbreaks with high attack rates, necessitating research into the factors regulating virus transmission[1]. The urban-dwelling mosquito *A. aegypti* serves as a particularly efficient vector because it feeds predominately and frequently on human hosts (every 2–3 d), thereby increasing the frequency of host contact[7–13]. Nevertheless, in laboratory trials, *A. aegypti* populations from endemic regions often exhibit unexpectedly low vector competence values for their arboviruses, as measured by the proportion of mosquitoes that become infected and transmit a pathogen after ingesting virus[14–18]. This could be explained, in part, by the techniques used to assess vector competence. In these studies, mosquitoes were offered an initial infectious blood meal and not allowed to refeed on blood again before assaying them for virus transmission, as is standard practice for assessing vector competence. Therefore, these studies do not recapitulate the natural biology of mosquitoes that refeed frequently. It is possible that differences in feeding history could help explain the seemingly paradoxical nature of *A. aegypti*-transmitted arboviruses.

Once a mosquito ingests an infected blood meal, arboviruses must overcome multiple barriers within the mosquito for transmission to occur[19]. The virus must infect the midgut, disseminate out of midgut cells, traverse the basal lamina layer to the haemolymph and then infect the salivary glands before being transmitted to the next vertebrate host[20]. Failure of virus escape out of the mosquito midgut to the peripheral tissues has been identified as an important barrier to arbovirus transmission, but the underlying factors mediating this process are poorly understood[14,15,21–23]. Blood feeding triggers physiological changes within the mosquito—including mechanical distention of the midgut, apoptosis and regeneration of midgut epithelial cells, and altered permeability of the basal lamina—that could enhance or accelerate virus dissemination out of the midgut[24–27]. On the basis these considerations, we evaluated the hypothesis that virus-infected mosquitoes fed an additional non-infectious blood meal will more effectively disseminate and transmit virus than mosquitoes fed only once.

To test this hypothesis, we provided *A. aegypti* with a second non-infectious blood meal 3 d after the infectious blood meal and compared virus infection and dissemination rates to those of mosquitoes that received a single blood meal (Fig. 1a). Midgut infection prevalence of ZIKV was similar in the single- and double-feed groups, but the percentage of mosquitoes with disseminated ZIKV infection to leg tissues was significantly higher in mosquitoes

[1]Center for Vector-Borne and Zoonotic Diseases, Department of Environmental Sciences, The Connecticut Agricultural Experiment Station, New Haven, CT, USA. [2]Department of Epidemiology of Microbial Diseases, Yale School of Public Health, Yale University, New Haven, CT, USA. [3]Department of Microbiology, Immunology and Pathology, Colorado State University, Fort Collins, CO, USA. [4]Department of Biomedical Sciences, Quinnipiac University, Hamden, CT, USA. [5]Department of Biostatistics, Yale School of Public Health, Yale University, New Haven, CT, USA. *e-mail: philip.armstrong@ct.gov; doug.brackney@ct.gov

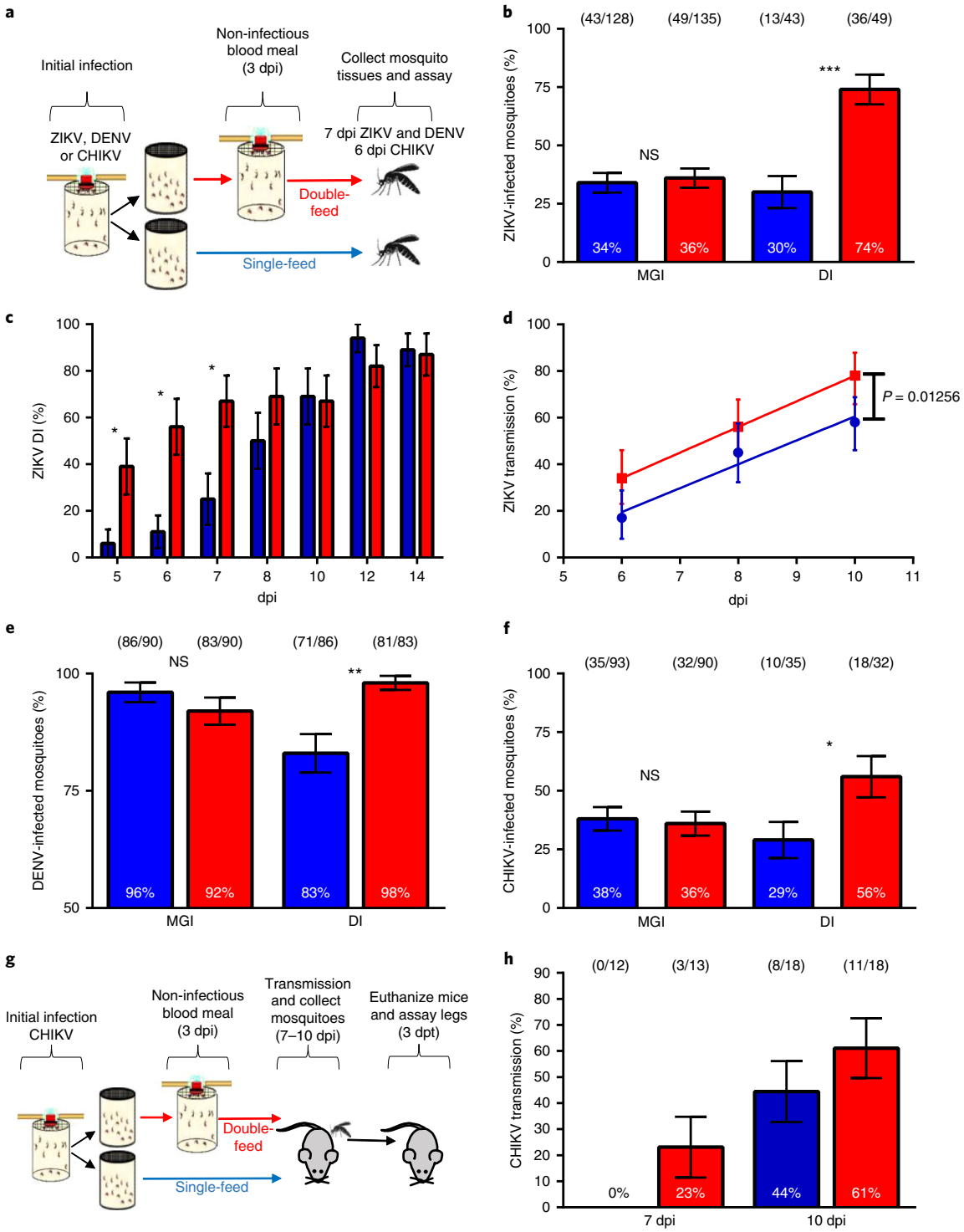


**Fig. 1 | Multiple feeding events increase dissemination and transmission rates of ZIKV, DENV and CHIKV in *A. aegypti*.** **a**, A schematic of the experimental design. **b**, At 7 dpi, paired bodies and legs were collected and assayed for the presence of ZIKV RNA by RT–qPCR. **c**, ZIKV dissemination rates of paired bodies and legs at 5–14 dpi assayed for ZIKV RNA; only DI rates are presented. **d**, 6, 8 and 10 dpi paired bodies and saliva were assayed for ZIKV RNA; only transmission rates are presented. Transmission rate data were analysed by linear regression and analysis of covariance. **e**,**f**, DENV-2 (**e**) and CHIKV (**f**) infection and dissemination rates. **g**, A schematic of the mouse transmission studies. dpt, days post transmission. **h**, The transmission rate of CHIKV-infected *A. aegypti* transmitting to suckling mice. Blue, single-feed; red, double-feed. The data were analysed by a two-sided Fisher's exact test. $^{*}P < 0.05$; $^{**}P < 0.01$; $^{***}P < 0.001$; NS, not significant. For **b**–**f**,**h**, horizontal lines and error bars represent the proportions and binomial s.e.m. of the sample proportions, respectively. *n* for each experiment and precise *P* values can be found in the source data.

receiving a second blood meal than those fed only once (Fig. 1b). Enhanced virus dissemination did not occur when mosquitoes were fed a non-infectious blood meal before receiving a ZIKV infectious blood meal (Extended Data Fig. 1). This suggests that an established midgut infection is a prerequisite for the observed enhanced rates of virus dissemination following a non-infectious blood meal.

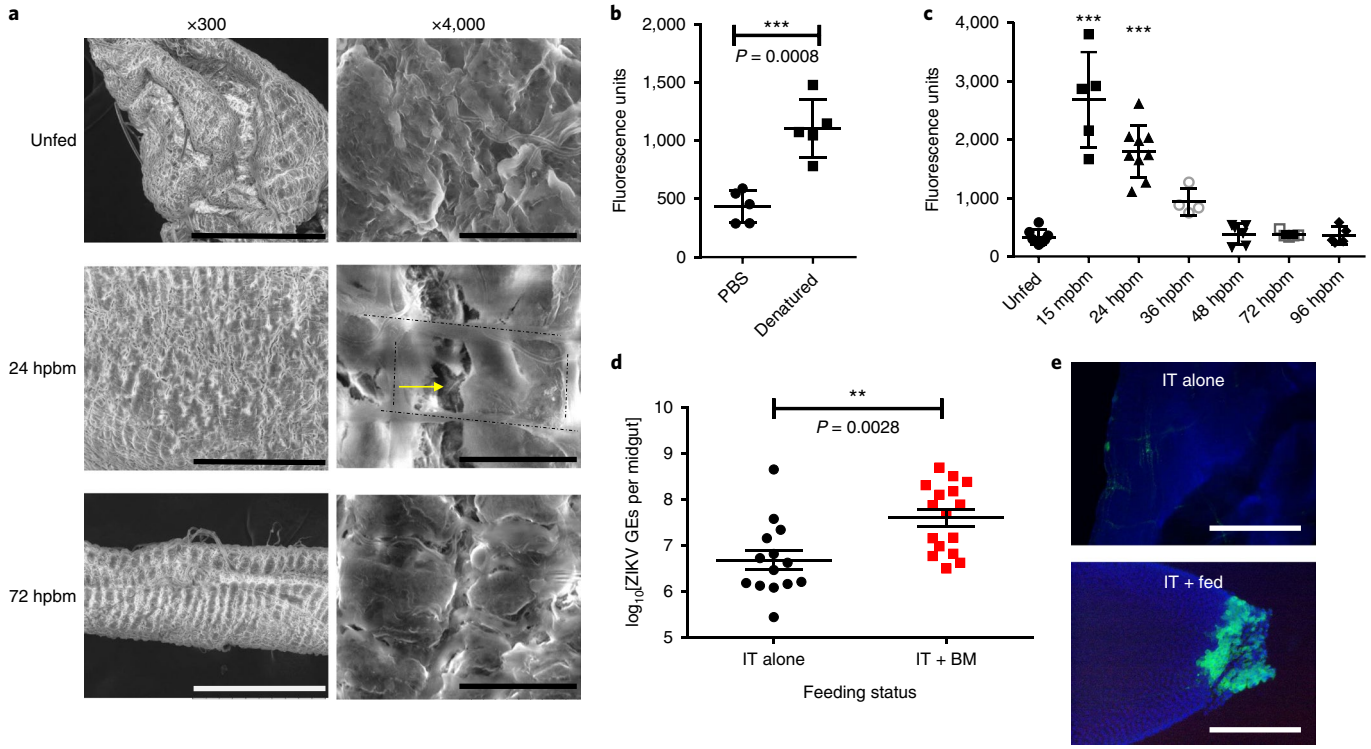


**Fig. 2 | Blood meal acquisition induces microperforations in the midgut basal lamina. a**, Representative scanning electron micrographs of naïve and engorged *A. aegypti* midguts at 24 hpbm and 72 hpbm at original magnification, ×300 (scale bars, 300 μm) and original magnification, ×4,000 (scale bars, 20 μm). The images are representative of two experimental replicates with five midguts per replicate. The black dashed lines outline the visceral musculature and the yellow arrow denotes microperforations in the underlying basal lamina. **b**, Pools of five unfed *A. aegypti* midguts per replicate were assayed for fluorescein-labelled CHP binding ($n=5$). Samples were analysed by two-tailed *t*-test ($P=0.0008$). **c**, The temporal binding profile of CHP binding to pools of five midguts per replicate following a single blood meal. Differences in CHP binding were determined using a one-way analysis of variance with a Dunnett's multiple comparisons post-hoc test. Precise *P* values and samples sizes can be found in the source data. **d**, Viral genome equivalents (GEs) per midgut of individuals intrathoracically inoculated (IT) with ZIKV ($n=14$) or inoculated and provided with a blood meal (BM) at 3 dpi ($n=16$). Midguts were assayed at 12 dpi by RT–qPCR and statistically analysed with a two-tailed *t*-test. **e**, Midguts from ZIKV-inoculated individuals with or without a blood meal assayed for ZIKV antigen at 12 dpi. Representative images of two experimental replicates of ten individual midguts per group are shown. Images were acquired at original magnification, ×200 (scale bars, 100 μm). For **b**–**d**, the horizontal lines represent the means and the error bars represent the s.d. $^{**}P<0.01$; $^{***}P<0.001$.

Temporal examination of this observation revealed that ZIKV disseminated more rapidly in the double-feed group than the single-feed group, but the difference in dissemination rates disappeared by day 10 post-infection (Fig. 1c). The increase in dissemination correlated with an increase of ZIKV-positive saliva samples as the transmission rate regression line elevations (*y* intercepts) were significantly different ($P=0.01256$) between the double-feed and single-feed cohorts, thus demonstrating enhanced early transmission potential (Fig. 1d and Extended Data Fig. 2). The dissemination and transmission studies were completed in different laboratories using different strains of *A. aegypti*, further demonstrating the robustness of the double-feed observation.

To assess the impact of mosquito refeeding on vector competency for other arboviruses, *A. aegypti* were orally exposed to DENV type 2 (DENV-2) and CHIKV and then given a second blood meal. As with ZIKV, the proportion of mosquitoes with disseminated infections (DIs) for both DENV-2 (Fig. 1e) and CHIKV (Fig. 1f) was significantly increased compared to single-feed controls. The increased dissemination rates associated with double-feeding resulted in a higher proportion of mosquitoes transmitting CHIKV to mice (Fig. 1h). This demonstrates that the serial feeding behaviour of *A. aegypti* enhances transmission of taxonomically diverse arboviruses and suggests that the mechanisms mediating this observation may be applicable to other virus–mosquito pairings.

To evaluate whether our findings were unique to *A. aegypti*, we tested ZIKV rates of dissemination in a low-generation ($F_5$) colony of *A. albopictus* that also refeeds within a single gonotrophic cycle[28,29]. As for *A. aegypti*, administration of a second non-infectious blood meal increased dissemination rates in *A. albopictus* (Extended Data Fig. 3). These findings suggest that under field conditions of frequent feeding, *A. albopictus* are more competent and could have contributed more to transmission during the ZIKV epidemic than previously thought.

To ascertain the basis of these findings, we determined whether an influx of energy-rich blood would promote viral replication and midgut escape. The number of virus genome equivalents was similar in mosquitoes regardless of feeding status (single- versus double-feed) or infection status (midgut-restricted infection versus DI) (Extended Data Fig. 4). Our data indicate that once ZIKV has established an infection in the gut, its ability to escape is not conditioned by enhanced viral replication. These findings are consistent with studies that found no correlation between midgut titres and dissemination rates[30,31] but contrast with the findings of Kramer et al. that showed higher midgut titres in mosquitoes with disseminated western equine encephalitis virus infection[32].

The midgut is encased in a proteoglycan extracellular matrix, termed the basal lamina, which provides protection and support to the epithelium. The pore size of the basal lamina is roughly 10 nm,

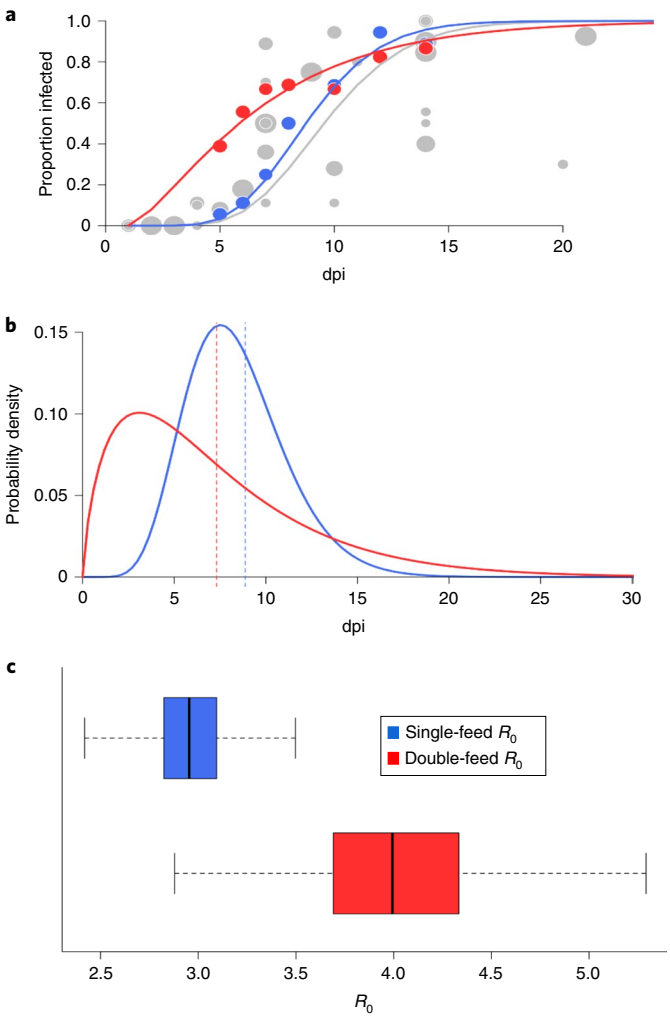


**Fig. 3 | Offering mosquitoes a second blood meal post-infection decreases the mean EIP and increases the transmission potential of ZIKV. a**, Data from our single-feed DI experiments (blue circles) and double-feed DI experiments (red circles) with the respective fitted gamma CDF (blue line, single-feed; red line, double-feed). Each data point represents the proportion of infected mosquitoes at a single time point in a given experiment; the radii correspond proportionally to both the sample size and weight in estimating the parameters of the CDF. For reference, we also estimated ZIKV dissemination rates in *A. aegypti* mosquitoes offered only one infectious blood meal based on data from seven published studies along with our own single-feed results (grey circles), and fitted a gamma CDF to the aggregated data (grey line). **b**, Posterior densities for the single-feed EIP (blue line) and double-feed EIP (red line) plotted with the corresponding means of the respective EIPs (dashed lines). **c**, The boxplots display the distribution of mean $R_0$ values for mosquitoes offered a single blood meal (blue) versus a second blood meal (red). The boxes represent the interquartile range of the mean $R_0$ values, the black line within the box marks the median and the whiskers indicate the 10th and 90th percentiles of the mean $R_0$ values.

yet the arboviruses tested in this study are 50–70 nm in size[33]. To determine whether blood-feeding alters basal lamina integrity, thereby accommodating transit of the larger virus particles, we performed scanning electron microscopy on *A. aegypti* midguts pre- and post-blood-meal. The basal lamina of unfed midguts appeared intact and ruffled, while the basal lamina of midguts at 24 h post-blood meal (hpbm) were distended and had clear signs of damage (Fig. 2a). By 72 hpbm, the integrity of the basal lamina was reconstituted. Temporal quantification of basal lamina damage was performed using a collagen hybridizing peptide (CHP) binding assay. CHP specifically binds to damaged collagen IV, a major component of the basal lamina (Fig. 2b). Consistent with the scanning electron microscopy data, the CHP binding assay revealed high degrees of binding within 15 min post-blood-meal (mpbm) and statistically significant elevated levels of binding up to 36 hpbm (Fig. 2c). By 48 hpbm, CHP binding levels had returned to pre-blood-fed levels, suggesting basal lamina repair. It has been proposed that blood-meal-induced basal lamina damage is due to enzymatic degradation[25]. However, our temporal data suggest that basal lamina damage is more likely the result of mechanical distention because it occurs immediately after blood engorgement. To evaluate how blood-meal-induced microperforations in the midgut basal lamina might affect virus transit, we performed a retrograde infection assay. ZIKV was intrathoracically inoculated into a cohort of *A. aegypti* and half were provided with a non-infectious blood meal at 3 d post-inoculation (dpi). At 9 d post-blood-meal, mosquito midguts were removed, ZIKV antigen was detected by immunofluorescence and ZIKV genome equivalents were quantified by quantitative PCR with reverse transcription (RT–qPCR). ZIKV titres were significantly higher in those provided with a blood meal (Fig. 2d) and clear signs of midgut epithelial infection could be detected in those provided with a blood meal, whereas ZIKV antigen could not be detected in the epithelium of non-blood-fed individuals (Fig. 2e). Together these data provide a likely mechanism by which arboviruses are able to disseminate from the mosquito midgut and explain how virus already seeded in the midgut can easily escape following acquisition of a second blood meal, while non-infectious blood meals provided before an infectious blood meal fail to enhance escape (Extended Data Fig. 1).

To quantify how a second blood meal would affect transmission of ZIKV by *A. aegypti* as measured by the basic reproductive number ($R_0$), we first modelled the distributions of the ZIKV EIP when mosquitoes were fed only one blood meal and again when they were fed a second non-infectious blood meal, using our experimental data on DI (Fig. 3a). We estimated the mean EIP to be 8.88 d (posterior standard deviation (PSD) = 2.94 d) when mosquitoes were fed only one blood meal and 7.33 d (PSD = 5.96 d) when mosquitoes were fed a second non-infectious blood meal (Fig. 3b). The posterior probability that the mean for the single-feed EIP $\left(\mu_{\mathrm{EIP_{SF}}}\right)$ was larger than that of the double-feed EIP $(\mu_{\mathrm{EIP_{DF}}})$ is 0.96 $\left(p\left(\mu_{\mathrm{EIP_{SF}}} > \mu_{\mathrm{EIP_{DF}}} | \mathrm{data}\right) = 0.96\right)$ (Extended Data Fig. 5). The results were similar for the salivary gland infection (SGI) data and when comparing our double-feed data to an estimate of the single-feed EIP derived from a meta-analysis of published studies that temporally assessed ZIKV infection rates (Fig. 3a).

On the basis of our single-feed empirical distribution of the EIP, we estimated the mean $R_{0_{\mathrm{SF}}}$ $\left(\mu_{R0_{\mathrm{SF}}}\right)$ to be 2.96 (95% credible interval (CI): 2.58–3.39), whereas when mosquitoes were fed a second blood meal following the initial infectious blood meal, the mean $R_{0_{\mathrm{DF}}}$ $\left(\mu_{R0_{\mathrm{DF}}}\right)$ was 4.05 (95% CI: 3.22–5.17) $\left(p\left(\mu_{R0_{\mathrm{DF}}} > \mu_{R0_{\mathrm{SF}}} | \mathrm{data}\right) = 0.99\right)$ (Fig. 3c). The distribution of $R_0$ values was consistent with published estimates based on seroprevalence and incidence data from different locations (Extended Data Fig. 6). The median difference in $R_0$ $\left(R_{0_{\mathrm{DF}}} - R_{0_{\mathrm{SF}}}\right)$ was 1.03 (95% CI: 0.15, 2.25). The EIP was the first- or second-most influential parameter affecting the difference in $R_0$ according to our two sensitivity analyses (Extended Data Fig. 7). The estimated increase in $R_0$ following a second blood meal may help explain the magnitude of *A. aegypti*-vectored ZIKV epidemics despite the relatively low competence observed experimentally (after a single infectious blood meal) for this vector. Furthermore, our model predicted a greater epidemic potential of ZIKV (as indicated by $R_0 > 1$) in regions where the daily probability of mosquito survival is lower

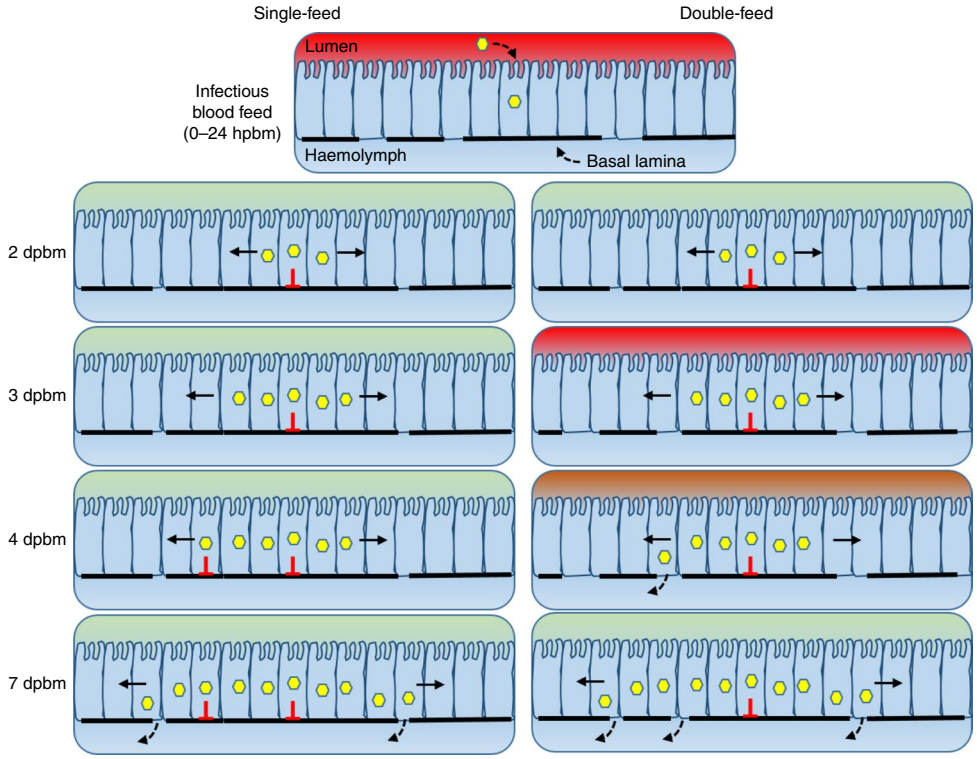


**Fig. 4 | Proposed model for double-feed-enhanced early dissemination and transmission.** As *Aedes* spp. mosquitoes acquire an infectious blood meal, the basal lamina underlying the midgut becomes compromised due to mechanical distention. Initially, only a few midgut cells become infected, but with time, viruses spread cell-to-cell, forming increasingly larger foci. Simultaneously, the basal lamina begins to partially repair. Eventually, the growing foci overlap with basal lamina microperforations, allowing viruses to bypass the basal lamina and enter the haemolymph. Acquisition of an additional blood meal would result in additional disruptions in the basal lamina, thereby increasing the likelihood that the growing virus foci will chance upon a break, resulting in earlier dissemination and transmission.

(Extended Data Fig. 8). Thus, the potential range of ZIKV persistence may be slightly greater than previously estimated[34].

This study establishes a connection between mosquito feeding behaviour and viral development within the vector that has direct impacts on the transmissibility and epidemic risk of arboviruses. We found that providing a second non-infectious blood meal to mosquitoes enhances viral dissemination from the midgut for a number of different virus–vector pairings. We propose that under field-relevant feeding regimens, viruses emerging from infected midgut epithelium cells can more readily traverse the basal lamina during subsequent feeding episodes as a result of blood-meal-induced microperforations (Fig. 4). During infection of the mosquito midgut, only a handful of cells are initially infected, but as the infection progresses, virus foci begin to expand, covering more of the midgut tissue[35]. If the initial infectious blood meal resulted in sporadic basal lamina disruption followed by partial repair, then growing virus foci will eventually overlap with regions of discontinuous basal lamina that could serve as a conduit for virus escape. The addition of a second blood meal would only increase the number of microperforations and thus increase the likelihood that virus foci will chance upon a basal lamina break before repair. This proposed model helps to explain how a second blood meal accelerates virus dissemination from an already established midgut infection.

One limitation of the current study concerns the use of artificial blood meals to feed mosquitoes. This method is commonly used for colony maintenance and for vector competence studies, and has advantages over the use of laboratory animals for convenience and for arboviruses such as ZIKV, DENV and CHIKV that do not produce infectious-level viraemias in easy to maintain animal hosts. Despite these advantages, the artificial feeding technique differs from natural blood feeding in ways that could potentially impact the results of this study. The technique requires the use of anticoagulated (defibrinated) blood that results in significantly lower arbovirus infection rates in mosquitoes than after feeding on viraemic hosts[36,37]. To overcome this impediment, ZIKV and DENV were grown in mosquito cell culture rather than mammalian cells to generate virus titres that were greater than observed during human viraemias. Viruses grown in insect cells express different *N*-linked glycan residues on the surface of the envelope protein that could also affect virus infection of the mosquito midgut[38]. Nevertheless, our study shows the impact of sequential blood meals on arbovirus dissemination from the gut after initial infection. This occurs long after the initial infectious blood meal is ingested and therefore the source of virus, virus titre and method of blood feeding are unlikely to alter our findings.

The volume of blood ingested during the second blood meal could potentially affect our results by impacting biophysical changes to the basal lamina layer surrounding the mosquito midgut. Most mosquitoes were fully engorged after blood feeding on a membrane feeder; however, in nature, blood feeding can often be interrupted, resulting in partial engorgement, which could influence virus dissemination associated with multiple feedings. A previous study found that collagen IV declined equally in the midguts of partially fed versus fully engorged mosquitoes[25]; however, it is unclear whether this reduction in collagen IV results in loss of basal lamina integrity or influences rates of dissemination. Further research is needed to evaluate the impact of blood meal volume on basal lamina integrity and virus dissemination rates to better understand the epidemiological significance of this phenomenon.

Taken together, our findings emphasize the importance of considering feeding behavioural traits when performing vector competence studies. Past studies may underestimate the risks of arbovirus transmission by measuring vector competence after only a single infectious blood meal.

## Methods

**Viruses, cell culture, mosquitoes and mice.** Viruses used in this study included ZIKV (PRVABC59; GenBank: KU501215), DENV-2 (125270/VENE93; GenBank: U91870) and CHIKV (R99659; GenBank: KX713902). C6/36 *A. albopictus* cells were used to amplify ZIKV (final passage history = Vero-3, C6/36-1) and DENV-2 (C6/36-3), CHIKV (Vero-2) were grown in Vero E6 cells, and BHK-21 (clone 15) cells were used to titrate infectious blood meals. Cell cultures were maintained in minimal essential medium with 10% fetal bovine serum, 100 U ml$^{-1}$ penicillin, 100 mg ml$^{-1}$ streptomycin, L-glutamine, 25 mg ml$^{-1}$ amphotericin B and sodium bicarbonate at 28 °C for C6/36 cells or 37 °C for Vero and BHK-21 cells with 5% $CO_2$. C6/36 and BHK-21 cells were confirmed to be clear of mycoplasma. Colonies of *A. aegypti* (Orlando strain, collected from Orlando, FL in 1952 and Poza Rica strain, collected from Poza Rica, Mexico in 2016) and *A. albopictus* (Stratford strain, generation $F_5$, collected in Stratford, CT, 2015) were maintained on defibrinated sheep's blood and reared under standard laboratory conditions[39]. Adult mosquitoes were housed at 27 °C in environmental chambers with a 14:10 light/dark cycle. Litters of suckling mice (mixed sex) from pregnant CD-1 mice were obtained from Charles River Laboratories. Statistical methods were not used to predetermine sample sizes. Litters of suckling mice were randomly assigned to cohorts of mosquitoes and individual suckling mice were randomly assigned to individual mosquitoes within the respective cohorts for the transmission studies. As for the mosquito samples, the right front leg of euthanized mice exposed to CHIKV-infected mosquitoes was collected by one group and provided to a second group for processing and data analysis. Group 2 was unaware of the order in which samples were given to them. Only after processing and data analysis were completed for each experimental replicate were Group 2 made aware of the sample order. Procedures for handling and care of animals were approved by and performed under the Animal Care and Use Committee at The Connecticut Agricultural Experiment Station (protocol no. P28-17).

**Vector competence studies.** *A. aegypti* and *A. albopictus* mosquitoes, 7–10 d post emergence, were offered an infectious blood meal containing a 1:1 mixture of defibrinated sheep's blood and virus. After feeding, mosquitoes were cold-anaesthetized and engorged females were transferred into two 32-oz ice cream cartons containing a small cup with an egg-laying paper and housed in a 27 °C environmental chamber. Mosquitoes had access to 10% sucrose sugar meals during the incubation period. Ingestion of sucrose was shown to be diverted to the mosquito crop rather than the midgut and, therefore, will have no expected impact on midgut expansion and basal lamina permeability[40].

At 3–7 d after the initial infectious blood meal, one of the two cartons was provided with a second non-infectious blood meal. Again, engorged females were collected and placed in a carton with a new egg-laying cup and provided access to 10% sucrose. Following variable EIPs, bodies, midguts, legs and salivary glands were collected and macerated in 250 µl PBS-G (phosphate-buffered saline with 0.5% gelatin, 30% rabbit serum and 1% 100× antibiotic–antimycotic (10,000 mg ml$^{-1}$ of streptomycin, 10,000 U ml$^{-1}$ penicillin and 25 mg ml$^{-1}$ of amphotericin B)) with a copper BB using a mixer mill. The inverse feeds (Extended Data Fig. 1) followed a similar experimental design; however, the double-feed group received a non-infectious blood meal before receiving a ZIKV-infectious blood meal. Either freshly grown virus or frozen virus stocks were used to complete the studies. Initially, all of the ZIKV studies were performed with frozen stocks of ZIKV ($4.8 \times 10^6$ plaque-forming units (p.f.u.) ml$^{-1}$); however, in light of the poor midgut infection rates, all subsequent experiments were performed with freshly grown virus ($1.0 \times 10^6$ –$10^7$ p.f.u. ml$^{-1}$); C6/36 cells were infected at a multiplicity of infection of ~0.1 and collected at 4–5 d post infection. While this change in protocol did increase midgut infection rates, it did not alter the enhanced dissemination rate phenotype associated with multiple blood meals. For comparison, mean human viraemia titres of ZIKV were estimated in the $10^4$–$10^5$ genome equivalents ml$^{-1}$ range[41,42]. DENV-2 was grown fresh on C6/36 cells ($5 \times 10^6$–$3 \times 10^7$ p.f.u. ml$^{-1}$) and frozen aliquots of CHIKV ($4 \times 10^6$ p.f.u. ml$^{-1}$) were used.

To evaluate ZIKV transmission by mosquitoes, saliva was collected in individual glass capillary tubes containing immersion oil type B. Salivation was allowed to occur for 25–30 min at room temperature. After salivation, the capillary tube was put into 100 µl Dulbecco's modified Eagle medium with 10% EquaFETAL (Atlas Biologicals) and 100 U ml$^{-1}$ penicillin and 100 µg ml$^{-1}$ streptomycin, and the tube was centrifuged at maximum speed for 5 min. Outbred mice are susceptible to CHIKV infection[43] and were used as host animals in CHIKV transmission experiments based on a previously published protocol[44]. Individual mosquitoes were allowed to feed on 5-d-old mice. Mice were euthanized 3 d after exposure to mosquitoes. The right front limb was removed from each mouse, homogenized in 500 µl PBS-G and tested for CHIKV infection by RT–qPCR.

Infection rates were determined and reported as follows. The midgut infection (MGI) rate represents the total number of virus-positive bodies divided by the total number of mosquitoes tested. Similarly, dissemination infection (DI) rates were determined by dividing the total number of virus-positive legs by the total number of virus-positive bodies. Transmission rates were calculated by dividing the total number of virus-positive salivary secretions or virus-positive recipient mice by the total number of virus-positive bodies.

**Viral RNA detection by RT–qPCR.** Total RNA was extracted from 50 µl of mosquito tissue and body homogenates using the Mag-Bind Viral DNA/RNA 96 Kit (Omega Bio-tek) on a Kingfisher Flex automated nucleic acid extraction device (ThermoFisher Scientific) following the manufacturer's instructions. Samples were eluted in 50 µl double-distilled $H_2O$. ZIKV RNA was detected in mosquito tissues using a previously described RT–qPCR primer–probe set (ZIKV 1087/1163c/1108 FAM)[45]. DENV-2 RNA was detected using a previously described primer–probe set spanning the 3′UTR[46] and CHIKV RNA was detected using the previously described 6856F/6981c/6919-FAM primer–probe set[47]. The same RT–qPCR protocol was used to detect all three viruses. In brief, 25 µl reactions containing 2.5 µl of total RNA were assayed with the TaqMan RNA-to-$C_t$ 1-Step Kit (ThermoFisher Scientific) on a CFX96 Touch Real-Time PCR Detection System (Bio-Rad) using the following parameters: RT—50 °C for 30 min, 95 °C for 10 min, PCR—95 °C for 15 s, 60 °C for 1 min followed by a plate read (50 cycles). Data were analysed using the Bio-Rad CFX Manager 3.1 software. The cutoff value used for ZIKV-exposed samples to be considered positive by RT–qPCR was $C_t < 37$. This cutoff value was empirically determined by comparing paired serial tenfold dilutions either inoculated on Vero cells or assayed by RT–qPCR (Supplementary Table 5). $C_t$ values <35 cycles were considered positive for CHIKV and <33 cycles for DENV-2. The use of RT–qPCR for scoring positives was validated by comparing RT–qPCR and cell culture isolation using salivary glands from ZIKV-exposed *A. aegypti*. While the percentage positive rate determined by RT–qPCR was higher, the difference in infection rates between single-feed and double-feed samples was maintained (Supplementary Table 6).

RNA standards were generated to quantify ZIKV RNA from mosquito midguts. Briefly, an ~680-base-pair fragment spanning the RT–qPCR primer set (positions 837–1520) was amplified with a forward primer containing a T7 promoter and a non-modified reverse primer. The amplicon was purified, sequenced and used as a template to generate RNA transcripts using the T7 Megascript Kit according to the manufacturer's instructions (ThermoFisher Scientific). RNA was quantified on a Qubit Fluorometer (ThermoFisher Scientific) and diluted to achieve serial tenfold genome equivalent dilutions. We detected $10^2$–$10^7$ ZIKV genome equivalents per reaction with a primer efficiency of 78.4% with an $R^2$ value of 0.971, a slope of −3.977 and a $y$ intercept = 46.965.

**Scanning electron microscopy.** *A. aegypti* mosquitoes, 7 d post emergence, were offered a non-infectious blood meal, sorted and housed as described in the main text. Ten midguts from unfed control and engorged mosquitoes were dissected at 24 and 72 hpbm and fixed in a 2% paraformaldehyde/2.5% glutaraldehyde solution containing 0.1% (w/v) $CaCl_2$ and 1% (w/v) sucrose buffered in 100 mM Na cacodylate (pH 7.3). Samples were fixed at 4 °C for 3 d and postfixed in 1% (w/v) $OsO_4$ in the same buffer at room temperature for 1 h. Fixed specimens were dehydrated through a graded ethanol and acetone series and imaged on a Hitachi Tabletop TM3030Plus scanning electron microscope.

**Collagen hybridizing peptide assay.** *A. aegypti* mosquitoes, 7 d post emergence, were provided a non-infectious blood meal. Midguts were temporally dissected from mosquitoes at 15 mpbm, 24 hpbm, 36 hpbm, 48 hpbm, 72 hpbm and 96 hpbm and fixed in a 2.5% glutaraldehyde and 2% paraformaldehyde solution for 24 h. Extra care was taken to not rupture engorged midguts during dissection. Baseline levels of CHP binding were determined with unfed midguts. Positive-control midguts included unfed midguts that were immediately heat denatured at 70 °C for 2 min before fixation. Midguts were grouped into five midguts per pool, each pool representing an experiential replicate of each time point. On fixation, midguts were washed three times in PBS and then incubated with fluorescein-labelled CHP (3Helix) diluted in PBS at a final concentration of 5 µM and incubated overnight at 4 °C. Subsequently, samples were washed three times in PBS and incubated with 1 µg µl$^{-1}$ elastase in PBS for 2 h at 27 °C and agitated every 15 min. Samples were transferred to a black 96-well plate ensuring that midguts were not transferred and diluted 1:1 with PBS. Fluorescence was determined on a BioTek SYNERGY H1 microplate reader using the area scan feature with and excitation/emission of 485/515 nm.

**Retrograde infection assay.** *A. aegypti* mosquitoes were intrathoracically inoculated with approximately 70 ZIKV p.f.u. At 3 dpi, half of the individuals were provided a non-infectious blood meal. Mosquitoes were housed for nine additional days, after which midguts were dissected. RNA was extracted and 15 samples from each group were assayed individually by RT–qPCR as described above. The remaining ten midguts were fixed in 4% paraformaldehyde overnight. Midguts were washed twice in PBS and stained with a 1:200 dilution of the mouse anti-flavivirus E-glycoprotein clone FE1 in blocking buffer (PBS + 5% BSA + 0.1%

Tween 20) and incubated for 1 h at room temperature. Midguts were washed three times in PBS + 0.1 Tween 20 and incubated with a donkey anti-mouse IgG conjugated to Alexafluor 488 diluted 1:200 in PBS + 0.1% Tween 20. Samples were washed three times in PBS + 0.1% Tween 20 and mounted on microscope slides with ProLong Gold Antifade with 4′,6-diamidino-2-phenylindole (DAPI).

**Statistical analysis of experimental data.** The data were pooled from two to four independent replicates for each experiment involving mosquitoes. Statistical methods were not used to predetermine sample size. Differences in the proportion of mosquitoes with midgut infection, DI or SGI were analysed using Fisher's exact test. Standard error bars were determined by calculating the standard error of sample proportions. ZIKV transmission rate data were analysed by linear regression and evaluated for differences in slope and $y$ intercept by analysis of covariance. Descriptive statistics are provided in the figure legends. All analyses were performed using GraphPad Prism statistical software.

**ZIKV plaque assay.** In addition to RT–qPCR, salivary secretions from ZIKV-infected *A. aegypti* were assayed by plaque assay to confirm the presence of infectious virus particles. Briefly, saliva from individual mosquitoes was diluted in cell culture medium and plated on sub-confluent monolayers of Vero cells. Cells were incubated for 1 h at 37 °C, after which a semi-solid medium overlay (Dulbecco's modified Eagle medium with 4% EquaFETAL, 2× Pen-Strep and 4 μg ml$^{-1}$ amphotericin B, mixed with an equal volume of 1.2% tragacanth gum) (EquaFETAL, Atlas Biologicals) (tragacanth, MP Biomedicals) was added. Cells were incubated for 4–5 d at 37 °C in 5% $CO_2$, and stained with crystal violet, and plaques were enumerated.

**Estimates of EIP distributions for ZIKV.** We developed models to estimate the distribution of the EIP of ZIKV under both single-feed and double-feed scenarios. As the exact moment when a mosquito becomes infectious is not observable, observations of EIP for a particular vector-borne disease are generally reported as a range of days from the time when some proportion of mosquitoes first exhibit dissemination of the virus into the body or salivary glands following an infectious blood meal, to the time where a maximum proportion of mosquitoes exhibit DI or transmission[48]. Whereas transmission studies often report the EIP as a range of days, we attempted to quantitatively describe the distribution of the EIP for ZIKV using our experimental results, and compare these results to published experimental data, to more accurately assess changes in the EIP when mosquitoes are offered a second blood meal during the incubation period.

Published data on the EIP of ZIKV were collected by searching the relevant literature using Web of Science, PubMed and Google Scholar; search terms included '*Aedes aegypti*' AND 'Zika' AND ('extrinsic incubation period' OR 'dissemination' OR 'salivary gland infection' OR 'competence' OR 'transmission'). We required that ZIKV infection data were collected on mosquitoes at three or more time points post-infection. Exclusions were not made based on language or date of publication. We attempted to account for sources of study variability (for example, ZIKV strain, utilization of fresh or frozen virus stock, and geographic origin of mosquitoes) in our models by incorporating a study-specific random effect. We identified nine papers in total that experimentally assessed ZIKV EIP in *A. aegypti* using traditional single-feed methodology (Supplementary Table 1). We aggregated DI rate data for studies in which temporal infection data were collected on ZIKV dissemination to legs, wings or heads, including our own single-feed experimental results. Separately, we aggregated SGI rate data for studies in which temporal infection data were collected on ZIKV dissemination to heads, salivary glands or in salivary secretions.

We assumed that the EIP for ZIKV was gamma distributed and that the data on the proportion of mosquitoes with DI sampled after $t$ days could be modelled according to a gamma cumulative distribution function (CDF)[48,49]. We used a Bayesian framework to obtain estimates needed to parameterize the EIP distribution for ZIKV according to the formula:

$$p_{t,i} = F_{\mathrm{EIP}}\left(t, \alpha_j, \beta_j + \varepsilon_i\right) = \frac{\left(\beta_j + \varepsilon_i\right)^{\alpha_j}}{\Gamma\left(\alpha_j\right)} \int_0^t u^{\alpha_j - 1} \mathrm{e}^{-\left(\beta_j + \varepsilon_i\right)u} \mathrm{d}u$$

where the gamma CDF is defined by the shape parameter $\alpha_j$ and the rate parameter $\beta_j$ for dataset $j$, with $j = 1$ for the single-feed data and $j = 2$ for the double-feed data; $\Gamma\left(\alpha_j\right)$ refers to the incomplete gamma function. We included an additional parameter $\varepsilon_i$ to account for inter-study variability when fitting the model to the DI and SGI meta-analysis data composed of observations from multiple studies. The observed number of mosquitoes with DI at time $t$ in experiment $i$ ($x_{t,i}$) was assumed to be binomially distributed with sample size ($n_{t,i}$) and a success probability ($p_{t,i}$):

$$x_{t,i} \sim \mathrm{binomial}\left(n_{t,i}, p_{t,i}\right)$$

We selected weakly informative priors for $\alpha_j$ (Gamma(0.001, 0.001)) and $\beta_j$ (log-normal(0, 0.001)), and assumed that $\varepsilon_i$ was normally distributed with mean 0 and variance $\tau$; again, we specified a weakly informative Gamma(0.001, 0.001) prior for $\tau$. Posterior distributions were estimated via a Markov chain Monte Carlo (MCMC) sampling algorithm implemented using JAGS, run from the statistical program R with the rjags package[50,51]. The algorithm was run for 100,000 iterations with 5,000 burn-in iterations for two chains. We fitted the model to six datasets: the single-feed dissemination data ($n = 7$ observations from our experimental results); the double-feed dissemination data ($n = 7$ observations from our experimental results); the single-feed salivary gland data ($n = 3$ observations from our experimental results); the double-feed salivary gland data ($n = 3$ observations from our experimental results); the meta-analysis single-feed dissemination data ($n = 38$ observations from 7 published studies aggregated with our single-feed dissemination results); and the meta-analysis single-feed salivary gland data ($n = 45$ observations from 8 published studies). Convergence was assessed through visual inspection of trace plots and calculation of the Gelman–Rubin convergence diagnostic (97.5% quantile of $\hat{R} < 1.1$) for all monitored parameters[52]. Using a thinned subset (10%) of each model's respective posterior shape and rate posterior distributions, we estimated the posterior distribution of mean EIP values as $E[\mathrm{EIP}] = \alpha/\beta$ and $\mathrm{Var}(\mathrm{EIP}) = \alpha/\beta^2$ for each iteration.

The models all showed clear indications of convergence, with a 97.5% quantile of $\hat{R} < 1.007$ for all monitored parameters. We first compared the estimated EIP for our experimental results based on the dissemination data to those based on the SGI data. The estimated EIPs were similar: $\mu_{\mathrm{EIP_{SD,DI}}} = 7.3$ d, $\mu_{\mathrm{EIP_{DF,SGI}}} = 7.8$ d, while $\mu_{\mathrm{EIP_{SF,DI}}} = 8.9$ d, $\mu_{\mathrm{EIP_{SF,SGI}}} = 9.7$ d. However, the variance in the posterior distributions based on the salivary gland data was considerably greater due to the limited number of data points ($n = 3$) (Supplementary Table 2). We then compared the model results for the meta-analysis DI and meta-analysis SGI datasets. We found the posterior means to be similar for DI ($\alpha_{1,\mathrm{DI}} = 3.89$ and $\beta_{1,\mathrm{DI}} = 0.34$) and SGI ($\alpha_{1,\mathrm{SGI}} = 3.78$ and $\beta_{1,\mathrm{SGI}} = 0.37$). We then compared model results for the meta-analysis DI and meta-analysis SGI datasets. We found the posterior means to be similar: $\alpha_{1\mathrm{dissem}} = 3.89$ and $\beta_{1,\mathrm{dissem}} = 0.34$ and $\alpha_{1,\mathrm{SGI}} = 3.78$ and $\beta_{1,\mathrm{SGI}} = 0.37$. However, the SGI data exhibited wider 95% CI and PSD of EIP ($\mu_{\mathrm{EIP_{SGI\_meta}}} = 10.82$ (95% CI: 5.65–19.20), $\sigma_{\mathrm{EIP_{SGI\_meta}}} = 5.60$ (95% CI: 2.82–10.10)) compared to the CI and PSD of EIP for the aggregated dissemination data ($\mu_{\mathrm{EIP_{dissem\_meta}}} = 10.17$ (95% CI: 7.12–14.07), $\sigma_{\mathrm{EIP_{dissem\_meta}}} = 5.19$ (95% CI: 3.58–7.40)). We also compared the aggregated single-feed dissemination data from the meta-analysis to our own single-feed dissemination data and found no significant difference in mean EIP estimates $\left(p\left(\mu_{\mathrm{EIP_{SF}}} > \mu_{\mathrm{EIP_{SF\_Meta}}} | \mathrm{data}\right) = 0.22\right)$.

We observed a large variability among studies in the literature on SGI rates over time (Extended Data Fig. 9) that did not appear to be attributable to the following study characteristics: mosquito strain, viral strain, viral titre, temperature or humidity during mosquito rearing, or fresh versus frozen viral stock. Notably, we observed a close similarity in posterior estimates of the mean EIP based on the dissemination and salivary gland data for both our experimental data and the meta-analysis (Supplementary Table 2). On the basis of these observations, as well as the fact that published studies exhibited more consistency in estimating dissemination rates (Fig. 3a), and we had considerably more experimental data points to fit to the model for dissemination to legs/wings than to the salivary glands, we chose to focus our subsequent analysis exclusively on the dissemination data.

Summary estimates of the posterior distributions of the mean EIP for the single- and double-feed data from this study, along with the aggregated single-feed data from our meta-analysis, are listed in Supplementary Table 2 and plotted in Fig. 3a,b for the dissemination data.

We assessed the difference in the distributions by calculating the posterior probability that the EIP for the double-feed data was greater than that of the single-feed data for the thinned subset of 20,000 random samples from the respective posterior distributions. The posterior probability that the aggregated mean single-feed EIP ($\mu_{\mathrm{EIP_{SF\_Meta}}}$) was greater than the mean double-feed EIP $\left(\mu_{\mathrm{EIP_{DF}}}\right)$ was 0.95; in other words, $\mu_{\mathrm{EIP_{DF}}}$ was less than or equal to $\mu_{\mathrm{EIP_{SF\_Meta}}}$ 5.0% of the time. The posterior probability that the single-feed EIP $\left(\mu_{\mathrm{EIP_{SF}}}\right)$ was greater than the double-feed EIP $\left(\mu_{\mathrm{EIP_{DF}}}\right)$ was 0.96 based on our experimental data; that is, $\mu_{\mathrm{EIP_{DF}}}$ was less than or equal to $\mu_{\mathrm{EIP_{SF}}}$ 4.2% of the time.

**Estimation of $R_0$.** To determine how the effect of multiple feeding episodes on EIP translates into the overall transmission potential of ZIKV, we estimated $R_0$ (defined as the average number of secondary human cases that a primary human case generates over the course of his or her infectious period in a fully susceptible population) under both single- and double-feed scenarios.

We estimated the basic reproductive number for the single-feed scenario $\left(R_{0_{\mathrm{SF}}}\right)$ according to the Ross–Macdonald model[53,54]:

$$R_{0_{\mathrm{SF}}} = \frac{m\, a^2 p^N b}{-\ln(p)} \times \frac{c}{r}$$

where $m$ is the ratio of mosquito to human population density, $a$ is the mosquito human-biting rate, $p$ is the probability of daily survival for mosquitoes, $b$ is the vector competence, $N$ is the EIP, $c$ is the probability that a mosquito is infected when biting an infectious human and $r$ is the human recovery rate. The first expression in the above equation represents the vectorial capacity, whereas the ratio $c/r$ represents the key human transmission parameters that dictate how the vectorial capacity relates to $R_0$ (ref. [54]). The biting rate $a$ is expressed intrinsically as the product of the time interval between blood meals and the proportion of mosquito blood meals on humans. Traditionally, and for our single-feed $R_0$, $a$ is

squared to account for the necessity of two bites to transmit infection from an infected to a susceptible human. To calculate $R_0$ for the double-feed data ($R_{0_{DF}}$), we modified this equation to examine the impact of an additional blood meal—which we assumed could come from an infected or uninfected human or non-human vertebrate—by multiplying by an additional factor $a/h$, where $h$ is the proportion of blood meals taken from humans:

$$R_{0_{DF}} = \frac{m a^2 \left(\frac{a}{h}\right) p^N b}{-\ln(p)} \times \frac{c}{r}$$

We parameterized our model for $R_0$ according to the current understanding of ZIKV transmission dynamics. When parameters specific to ZIKV transmission were not available or as yet understood, we informed the ranges from DENV studies, as ZIKV and DENV are arboviruses of the same *Flavivirus* genus, and are both spread by *Aedes* genus mosquitoes. Parameters were as specific as possible to *A. aegypti*, although ranges often accounted for what may also be observed with *A. albopictus*. As a conservative assumption (and consistent with our experimental finding that the difference in dissemination rates disappeared by day 10), we used values of the vector competence from the literature and assumed that $b$ did not vary between the single- and double-feed models. Parameter values and ranges are summarized in Supplementary Table 3. Parameter distributions are also specified, where triangular distributions signify the expectation that values close to the peak of the triangular distribution are more likely to occur (Supplementary Table 3).

To estimate how $R_0$ changes with feeding behaviour, we used our posterior distributions for the EIP as input into the above equations, since we assert that the EIP is better represented by a gamma distribution than a single static value. For each of a thinned subset (10%) of MCMC posterior samples of the shape and rate parameters, and for each model (single- and double-feed), we generated 20,000 gamma random variables as input to calculate 20,000 respective $R_0$ estimates. We then found the mean $R_0$ for that particular parameter set, and repeated this process for each MCMC sample in the subset. We then compared the distributions of the single- and double-feed $R_0$ defined by the respective EIP distributions.

On the basis of the single-feed distribution of the EIP for our experimental data, we estimated the mean $R_{0_{SF}}$ ($\mu_{R0_{SF}}$) to be 2.96 (95% CI: 2.58–3.39), whereas when mosquitoes were fed a second blood meal following the initial infectious blood meal, the mean $R_{0_{DF}}$ ($\mu_{R0_{DF}}$) was 4.05 (95% CI: 3.22–5.17) (Extended Data Fig. 5). The mean $R_{0_{DF}}$ was greater than the mean $R_{0_{SF}}$ for 99.0% of the posterior samples $\left(p\left(\mu_{R0_{DF}} > \mu_{R0_{SF}} | \text{data}\right) = 0.99\right)$. The median difference in $R_0$ estimates was 1.03 (95% CI: 0.15–2.25). We also estimated $\mu_{R0_{SF}\_Meta}$ to be 2.97 (95% CI: 1.84–4.29) based on the single-feed data from our meta-analysis, and found that the mean $R_{0_{DF}}$ was greater than the mean meta-analysis $R_{0_{SF}}$ for 92.0% of the posterior samples. Finally, we considered the threshold of $R_0 = 1$, above which an epidemic can occur in a susceptible population, and found that, on average, 94.1% of $R_{0_{SF}}$ estimates, 94.8% of $R_{0_{SF}\_Meta}$ estimates and 85.1% of $R_{0_{DF}}$ estimates were above this threshold.

We compared our estimates of $R_{0_{SF}}$ and $R_{0_{DF}}$ to estimates of $R_0$ from the literature. We identified 41 estimates of $R_0$ for ZIKV from 22 studies. Studies were identified by searching Web of Science and PubMed; search terms included 'Zika' AND ('reproductive OR reproduction number' OR 'R naught' OR 'R0' OR 'transmission potential' OR 'generation interval'). The estimates of $R_0$ calculated in this study fell within the range of published estimates based on field data (Extended Data Fig. 6). We also noted a wide variation in estimates of the generation interval of ZIKV (Supplementary Table 4), which is positively correlated with estimates of $R_0$ and has been shown to be a major source of uncertainty in $R_0$ estimates for ZIKV[55,56]. Our results suggest that estimates of the generation interval of ZIKV based on natural history models may be upwardly biased, since they rely on estimates of the EIP based on single-feed experimental data. Thus, estimates of $R_0$ based on fitting to case report data may also be slightly upwardly biased. However, uncertainty in the generation interval used to estimate $R_0$ in the literature is much greater than the difference in the EIP that we estimated for the single-feed and double-feed experimental data.

**Sensitivity analyses.** We assessed the sensitivity of the basic reproductive number estimates that resulted from variability in the input parameters $N$, $a$, $m$, $b$, $p$ and $h$ using two analyses. First, using a best/worst-case scenario approach, we held all parameters at their given or mean value (Supplementary Table 3) and calculated the difference in $R_0$ between single feed and double feeds, $(R_{0_{DF}} - R_{0_{SF}}) = 0.71$. We then varied each parameter individually according to the lowest and highest values in its specified range while holding all other parameters constant at their mean or given value (Supplementary Table 3) and assessed how the difference in $R_0$ between double- and single-feed estimates changed in magnitude from the initial difference. For the EIP estimates ($N$), we used our model results from the single-feed meta-analysis data because we felt they better represented the known variability in the distribution of EIP, as supported by numerous aggregated studies in addition to our own data. We found the most sensitive parameters to be the human-biting rate ($a$), the EIP ($N$) and the mosquito density ($m$) according to this analysis (Extended Data Fig. 7a).

Next, for each parameter, we randomly sampled from its specified distribution (Supplementary Table 3) while holding all other parameters constant at their mean or given value. For example, we took 10,000 random samples of $m$ from the Unif(1,10) distribution as input for both the single-feed and double-feed transmission models and then examined the distribution of differences in $R_0$ ($R_{0_{DF}} - R_{0_{SF}}$) for each of the 10,000 iterations (Extended Data Fig. 7b). According to this analysis, we found the three most sensitive parameters to be the EIP ($N$), the human-biting rate ($a$) and the probability of daily survival for mosquitoes ($p$), in that order. This analysis also sheds light on the anomalous behaviour of $p$; although random sampling generally resulted in $R_{0_{DF}} > R_{0_{SF}}$, the long tail of the distribution of differences suggests that a minority (14.4%) of random samples of $p$ resulted in $R_{0_{DF}} < R_{0_{SF}}$, and the majority of samples resulted in a difference less than the constant $(R_{0_{DF}} - R_{0_{SF}})$ difference of 0.71. The largest values of $(R_{0_{DF}} - R_{0_{SF}})$ resulted from samples of $p$ in the middle of its range.

We also plotted the relationship between $R_0$ and $p$ (that is, the probability of daily survival of mosquitoes), as this parameter plays an important role in the variability of $R_0$ across different climates (Extended Data Fig. 8). For each value of $p$ specified in Supplementary Table 3, we generated 10,000 gamma-distributed estimates of the EIP as input to calculate 10,000 respective $R_0$ estimates, as previously described. At high values of $p$, $R_0$ is slightly larger for the single-feed model, although the overall magnitude of $R_0$ for either model is large and unlikely to be observed in a natural setting. At lower values of $p$, within the range where ZIKV epidemics have been observed, $R_0$ is slightly higher under the double-feed model (Extended Data Fig. 8a) and is more likely to be greater than 1 (Extended Data Fig. 8b). Our results therefore suggest that multiple blood meals in a natural setting may lead to greater persistence of ZIKV on the edges of observed transmission zones.

Finally, we performed a full probabilistic uncertainty analysis where we estimated the total uncertainty of the mean difference in $R_0$ between single- and double-feeds using Latin hypercube sampling. With this approach, we created a matrix of uniform random output of 10,000 samples using the R software randomLHS function as input to the quantile function for each parameter's specified distribution (Supplementary Table 3)[57]. We then determined the distribution of $R_0$ values and removed those outside the 95% CI to maintain realistic estimates. The $R_{0_{SF}}$ and $R_{0_{DF}}$ histograms are shown in Extended Data Fig. 10a. The two $R_0$ distributions overlap significantly, but the mean value for $R_{0_{DF}}$ is larger than that of $R_{0_{SF}}$. The distribution of $(R_{0_{DF}} - R_{0_{SF}})$ for each random sample is shown in Extended Data Fig. 10b. The distribution is skewed slightly to the right with a mean difference of 0.87. Note that in this analysis, we are implicitly assuming that all of the parameters—including the EIP for the single- and double-feed models—are independent of one another, which is unlikely to be the case, but covariance of the different parameters is unknown.

**Reporting Summary.** Further information on research design is available in the Nature Research Reporting Summary linked to this article.

## Data availability

Numerical source data underlying the graphs shown in Figs. 1 and 2c are associated with each figure. Additional data that support the findings of this study are available from the corresponding author upon request.

Received: 10 May 2019; Accepted: 23 October 2019;
Published online: 09 December 2019

## References

1. Mayer, S. V., Tesh, R. B. & Vasilakis, N. The emergence of arthropod-borne viral diseases: a global prospective on dengue, chikungunya and Zika fevers. *Acta Trop.* **166**, 155–163 (2017).
2. Faria, N. R. et al. Establishment and cryptic transmission of Zika virus in Brazil and the Americas. *Nature* **546**, 406–410 (2017).
3. Kramer, L. D. & Ciota, A. T. Dissecting vectorial capacity for mosquito-borne viruses. *Curr. Opin. Virol.* **15**, 112–118 (2015).
4. Scott, T. W. & Takken, W. Feeding strategies of anthropophilic mosquitoes result in increased risk of pathogen transmission. *Trends Parasitol.* **28**, 114–121 (2012).
5. Weaver, S. C. & Reisen, W. K. Present and future arboviral threats. *Antiviral Res.* **85**, 328–345 (2010).
6. Musso, D. & Gubler, D. J. Zika virus. *Clin. Microbiol. Rev.* **29**, 487–524 (2016).
7. Scott, T. W. et al. Blood-feeding patterns of *Aedes aegypti* (Diptera: Culicidae) collected in a rural Thai village. *J. Med. Entomol.* **30**, 922–927 (1993).
8. Scott, T. W. et al. Longitudinal studies of *Aedes aegypti* (Diptera: Culicidae) in Thailand and Puerto Rico: blood feeding frequency. *J. Med. Entomol.* **37**, 89–101 (2000).
9. Ponlawat, A. & Harrington, L. C. Blood feeding patterns of *Aedes aegypti* and *Aedes albopictus* in Thailand. *J. Med. Entomol.* **42**, 844–849 (2005).
10. Baak-Baak, C. M. et al. Blood feeding status, gonotrophic cycle and survivorship of *Aedes* (*Stegomyia*) *aegypti* (L.) (Diptera: Culicidae) caught in churches from Merida, Yucatan, Mexico. *Neotrop. Entomol.* **46**, 622–630 (2017).
11. Sivan, A., Shriram, A. N., Sunish, I. P. & Vidhya, P. T. Host-feeding pattern of *Aedes aegypti* and *Aedes albopictus* (Diptera: Culicidae) in heterogeneous landscapes of South Andaman, Andaman and Nicobar Islands, India. *Parasitol. Res.* **114**, 3539–3546 (2015).

12. De Benedictis, J. et al. Identification of the people from whom engorged *Aedes aegypti* took blood meals in Florida, Puerto Rico, using polymerase chain reaction-based DNA profiling. *Am. J. Trop. Med. Hyg.* **68**, 437–446 (2003).
13. Barrera, R. et al. Vertebrate hosts of *Aedes aegypti* and *Aedes mediovittatus* (Diptera: Culicidae) in rural Puerto Rico. *J. Med. Entomol.* **49**, 917–921 (2012).
14. Diagne, C. T. et al. Potential of selected Senegalese *Aedes* spp. mosquitoes (Diptera: Culicidae) to transmit Zika virus. *BMC Infect. Dis.* **15**, 492 (2015).
15. Chouin-Carneiro, T. et al. Differential susceptibilities of *Aedes aegypti* and *Aedes albopictus* from the Americas to Zika virus. *PLoS Negl. Trop. Dis.* **10**, e0004543 (2016).
16. Diagne, C. T. et al. Vector competence of *Aedes aegypti* and *Aedes vittatus* (Diptera: Culicidae) from Senegal and Cape Verde archipelago for West African lineages of chikungunya virus. *Am. J. Trop. Med. Hyg.* **91**, 635–641 (2014).
17. Calvez, E. et al. Dengue-1 virus and vector competence of *Aedes aegypti* (Diptera: Culicidae) populations from New Caledonia. *Parasites Vector* **10**, 381 (2017).
18. Diallo, M. et al. Vector competence of *Aedes aegypti* populations from Senegal for sylvatic and epidemic dengue 2 virus isolated in West Africa. *Trans. R. Soc. Trop. Med. Hyg.* **102**, 493–498 (2008).
19. Black, W. Ct et al. Flavivirus susceptibility in *Aedes aegypti*. *Arch. Med. Res.* **33**, 379–388 (2002).
20. Hardy, J. L. in *The Arboviruses: Epidemiology and Ecology* Vol. 1 (ed. Monath, T. P.) 87–126 (CRC, 1988).
21. Franz, A. W., Kantor, A. M., Passarelli, A. L. & Clem, R. J. Tissue barriers to arbovirus infection in mosquitoes. *Viruses* **7**, 3741–3767 (2015).
22. Vazeille, M., Dehecq, J. S. & Failloux, A. B. Vectorial status of the Asian tiger mosquito *Aedes albopictus* of La Reunion Island for Zika virus. *Med. Vet. Entomol.* **32**, 251–254 (2018).
23. O'Donnell, K. L., Bixby, M. A., Morin, K. J., Bradley, D. S. & Vaughan, J. A. Potential of a northern population of *Aedes vexans* (Diptera: Culicidae) to transmit Zika virus. *J. Med. Entomol.* **54**, 1354–1359 (2017).
24. Okuda, K. et al. Cell death and regeneration in the midgut of the mosquito, *Culex quinquefasciatus*. *J. Insect Physiol.* **53**, 1307–1315 (2007).
25. Dong, S. et al. Chikungunya virus dissemination from the midgut of *Aedes aegypti* is associated with temporal basal lamina degradation during bloodmeal digestion. *PLoS Negl. Trop. Dis.* **11**, e0005976 (2017).
26. Kantor, A. M., Grant, D. G., Balaraman, V., White, T. A. & Franz, A. W. E. Ultrastructural analysis of chikungunya virus dissemination from the midgut of the yellow fever mosquito, *Aedes aegypti*. *Viruses* **10**, 571 (2018).
27. Weaver, S. C., Scott, T. W., Lorenz, L. H., Lerdthusnee, K. & Romoser, W. S. Togavirus-associated pathologic changes in the midgut of a natural mosquito vector. *J. Virol.* **62**, 2083–2090 (1988).
28. Delatte, H. et al. Blood-feeding behavior of *Aedes albopictus*, a vector of Chikungunya on La Reunion. *Vector-Borne Zoonotic Dis.* **10**, 249–258 (2010).
29. Egizi, A., Healy, S. P. & Fonseca, D. M. Rapid blood meal scoring in anthropophilic *Aedes albopictus* and application of PCR blocking to avoid pseudogenes. *Infect. Genet. Evol.* **16C**, 122–128 (2013).
30. Dickson, L. B., Sanchez-Vargas, I., Sylla, M., Fleming, K. & Black, W. C. 4th Vector competence in West African *Aedes aegypti* is flavivirus species and genotype dependent. *PLoS Negl. Trop. Dis.* **8**, e3153 (2014).
31. Bosio, C. F., Beaty, B. J. & Black, W. C. 4th Quantitative genetics of vector competence for dengue-2 virus in *Aedes aegypti*. *Am. J. Trop. Med. Hyg.* **59**, 965–970 (1998).
32. Kramer, L. D., Hardy, J. L., Presser, S. B. & Houk, E. J. Dissemination barriers for western equine encephalomyelitis virus in *Culex tarsalis* infected after ingestion of low viral doses. *Am. J. Trop. Med. Hyg.* **30**, 190–197 (1981).
33. Houk, E. J., Hardy, J. L. & Chiles, R. E. Permeability of the midgut basal lamina in the mosquito, *Culex tarsalis* Coquillett (Insecta, Diptera). *Acta Trop.* **38**, 163–171 (1981).
34. Perkins, T. A., Siraj, A. S., Ruktanonchai, C. W., Kraemer, M. U. G. & Tatem, A. J. Model-based projections of Zika virus infections in childbearing women in the Americas. *Nat. Microbiol.* **1**, 16126.
35. Salazar, M. I., Richardson, J. H., Sanchez-Vargas, I., Olson, K. E. & Beaty, B. J. Dengue virus type 2: replication and tropisms in orally infected *Aedes aegypti* mosquitoes. *BMC Microbiol.* **7**, 9 (2007).
36. Meyer, R. P., Hardy, J. L. & Presser, S. B. Comparative vector competence of *Culex tarsalis* and *Culex quinquefasciatus* from the Coachella, Imperial, and San Joaquin Valleys of California for St. Louis encephalitis virus. *Am. J. Trop. Med. Hyg.* **32**, 305–311 (1983).
37. Turell, M. J. Reduced Rift Valley fever virus infection rates in mosquitoes associated with pledget feedings. *Am. J. Trop. Med. Hyg.* **39**, 597–602 (1988).
38. Hsieh, P. & Robbins, P. W. Regulation of asparagine-linked oligosaccharide processing. Oligosaccharide processing in *Aedes albopictus* mosquito cells. *J. Biol. Chem.* **259**, 2375–2382 (1984).
39. Armstrong, P. M. & Rico-Hesse, R. Differential susceptibility of *Aedes aegypti* to infection by the American and Southeast Asian genotypes of dengue type 2 virus. *Vector-Borne Zoonotic Dis.* **1**, 159–168 (2001).
40. Airs, P. M., Kudrna, K. E. & Bartholomay, L. C. Impact of sugar composition on meal distribution, longevity, and insecticide toxicity in *Aedes aegypti*. *Acta Trop.* **191**, 221–227 (2019).
41. Waggoner, J. J. et al. Viremia and clinical presentation in Nicaraguan patients infected with Zika virus, chikungunya virus, and dengue virus. *Clin. Infect. Dis.* **63**, 1584–1590 (2016).
42. Musso, D. et al. Molecular detection of Zika virus in blood and RNA load determination during the French Polynesian outbreak. *J. Med. Virol.* **89**, 1505–1510 (2017).
43. Haese, N. N. et al. Animal models of Chikungunya virus infection and disease. *J. Infect. Dis.* **214**, S482–S487 (2016).
44. Anderson, J. F., Main, A. J., Delroux, K. & Fikrig, E. Extrinsic incubation periods for horizontal and vertical transmission of West Nile virus by *Culex pipiens pipiens* (Diptera: Culicidae). *J. Med. Entomol.* **45**, 445–451 (2008).
45. Lanciotti, R. S. et al. Genetic and serologic properties of Zika virus associated with an epidemic, Yap State, Micronesia, 2007. *Emerg. Infect. Dis.* **14**, 1232–1239 (2008).
46. Alm, E. et al. Universal single-probe RT-PCR assay for diagnosis of dengue virus infections. *PLoS Negl. Trop. Dis.* **8**, e3416 (2014).
47. Lanciotti, R. S. et al. Chikungunya virus in US travelers returning from India, 2006. *Emerg. Infect. Dis.* **13**, 764–767 (2007).
48. Chan, M. & Johansson, M. A. The incubation periods of Dengue viruses. *PLoS ONE* **7**, e50972 (2012).
49. Ferguson, N. M. et al. Countering the Zika epidemic in Latin America. *Science* **353**, 353–354 (2016).
50. Plummer, M. rjags: Bayesian Graphical Models using MCMC. R package version 4-8 (2018).
51. *R: A Language and Environment for Statistical Computing* (R Foundation for Statistical Computing, 2014); http://www.R-project.org
52. Brooks, S. P. & Gelman, A. General methods for monitoring convergence of iterative simulations. *J. Comput. Graph. Stat.* **7**, 434–455 (1998).
53. Christofferson, R. C. & Mores, C. N. Estimating the magnitude and direction of altered arbovirus transmission due to viral phenotype. *PLoS ONE* **6**, e16298 (2011).
54. Smith, D. L. et al. Ross, Macdonald, and a theory for the dynamics and control of mosquito-transmitted pathogens. *PLoS Pathog.* **8**, e1002588 (2012).
55. Chowell, G. et al. Using phenomenological models to characterize transmissibility and forecast patterns and final burden of Zika epidemics. *PLoS Currents* https://doi.org/10.1371/currents.outbreaks.f14b2217c902f453d9320a43a35b9583 (2016).
56. Funk, S. et al. Comparative analysis of dengue and Zika outbreaks reveals differences by setting and virus. *PLoS Negl. Trop. Dis.* **10**, e0005173 (2016).
57. Carnell, R. lhs: Latin Hypercube Samples. R package version 1.0.1 (2019).


## Acknowledgements

We thank M. C. Thomas, M. Olson, T. Petruff and M. Correa who provided technical assistance with rearing, processing and virus testing of mosquitoes. This publication was supported by the Cooperative Agreement Number U01CK000509, funded by the Centers for Disease Control and Prevention. Its contents are solely the responsibility of the authors and do not necessarily represent the official views of the Centers for Disease Control and Prevention or the Department of Health and Human Services. This work was further supported by the US Department of Agriculture Hatch Funds and Multistate Research Project (CONH00773 and NE1443), the National Center for Advancing Translational Sciences of the National Institutes of Health (CTSA grant number UL1 TR001863 and KL2 TR001862) (J.L.W.) and the National Institutes of Health/National Institute of Allergy and Infectious Diseases (R01 AI112970) (V.E.P.) and R21 AI129464 (B.D.F.).

## Author contributions

P.M.A., H.Y.E., V.E.P. and D.E.B. conceived and designed the experiments and wrote the manuscript. P.M.A., D.E.B., T.M., M.R.M., B.D.F., A.B., M.J.M. and A.G.-S. performed mosquito experiments including mosquito infections, dissections, transmission assays and the quantification of viral RNA and infectious virus particles. D.E.B. performed the retrograde infection assay and fluorescence microscopy. P.J.C. performed the CHP assay. J.J.S. and T.G.A. performed the scanning electron microscopy. P.M.A. and D.E.B. statistically analysed and interpreted the experimental data. H.Y.E., J.L.W. and V.E.P. performed the modelling and statistics associated with the modelling. P.M.A., V.E.P., B.D.F. and D.E.B. oversaw the project.

## Competing interests

The authors declare no competing interests.

## Additional information

**Extended data** is available for this paper at https://doi.org/10.1038/s41564-019-0619-y.

**Supplementary information** is available for this paper at https://doi.org/10.1038/s41564-019-0619-y.

**Correspondence and requests for materials** should be addressed to P.M.A. or D.E.B.

**Reprints and permissions information** is available at www.nature.com/reprints.

**Publisher's note** Springer Nature remains neutral with regard to jurisdictional claims in published maps and institutional affiliations.

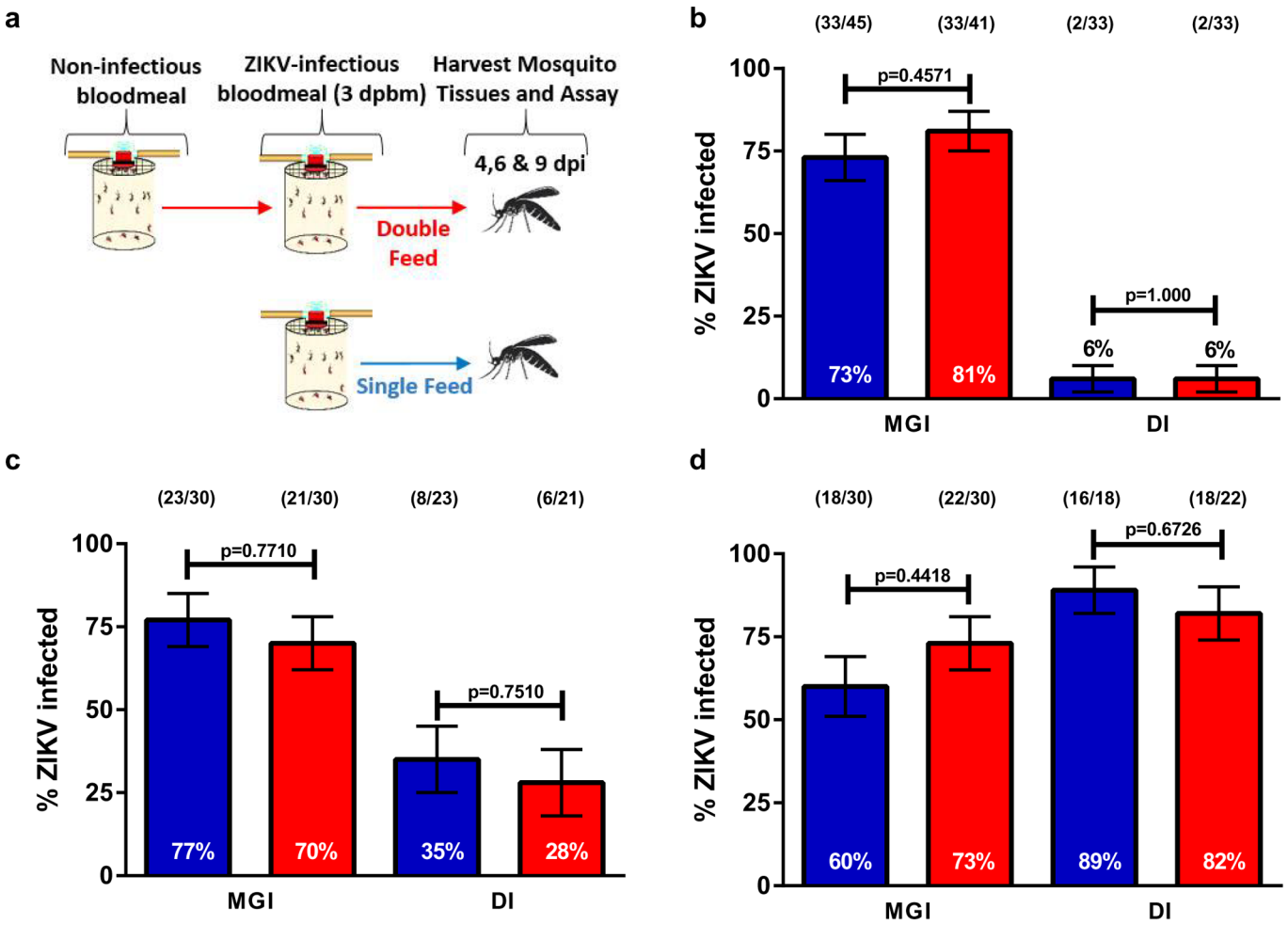


**Extended Data Fig. 1 | Non-infectious bloodmeals prior to infectious bloodmeals do not increase dissemination rates.** (a) Schematic of experimental design. At (b) 4, (c) 6, and (d) 9 dpi, midguts and legs were dissected from both cohorts and tested for the presence of ZIKV RNA by RT-qPCR. (●) single feed; (●) double feed. Data were analyzed by Two-sided Fisher's exact test. Sample sizes (represented as a fraction of positive samples/ total samples) for each treatment/ timepoint are embedded in the figures above each experimental group. Center values represent the proportion and error bars represent the binomial SE of sample proportions.

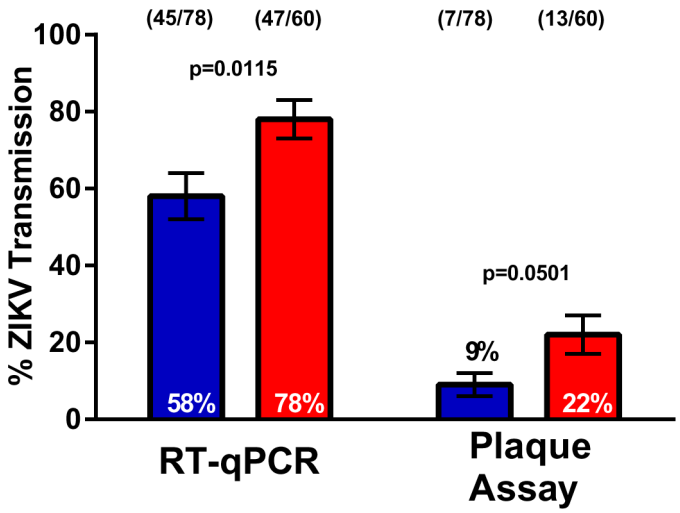


**Extended Data Fig. 2 | Increased transmission of ZIKV RNA and infectious virions associated with acquisition of an additional non-infectious bloodmeal.** *Aedes aegypti* mosquitoes were offered a ZIKV infectious bloodmeal and at 3 dpi individuals in the double-feed groups were fed a second, non-infectious bloodmeal. 10 dpi mosquito saliva was collected and assayed for ZIKV RNA and infectious virions by RT-qPCR and plaque assay respectively. (●) single feed; (●) double feed. Data were analyzed by Two-sided Fisher's exact test. (*) $p<0.05$. Sample sizes (represented as a fraction of positive samples/ total samples) for each treatment/ timepoint are embedded in the figures above each experimental group. Center values represent the proportion and error bars represent the binomial SE of sample proportions.

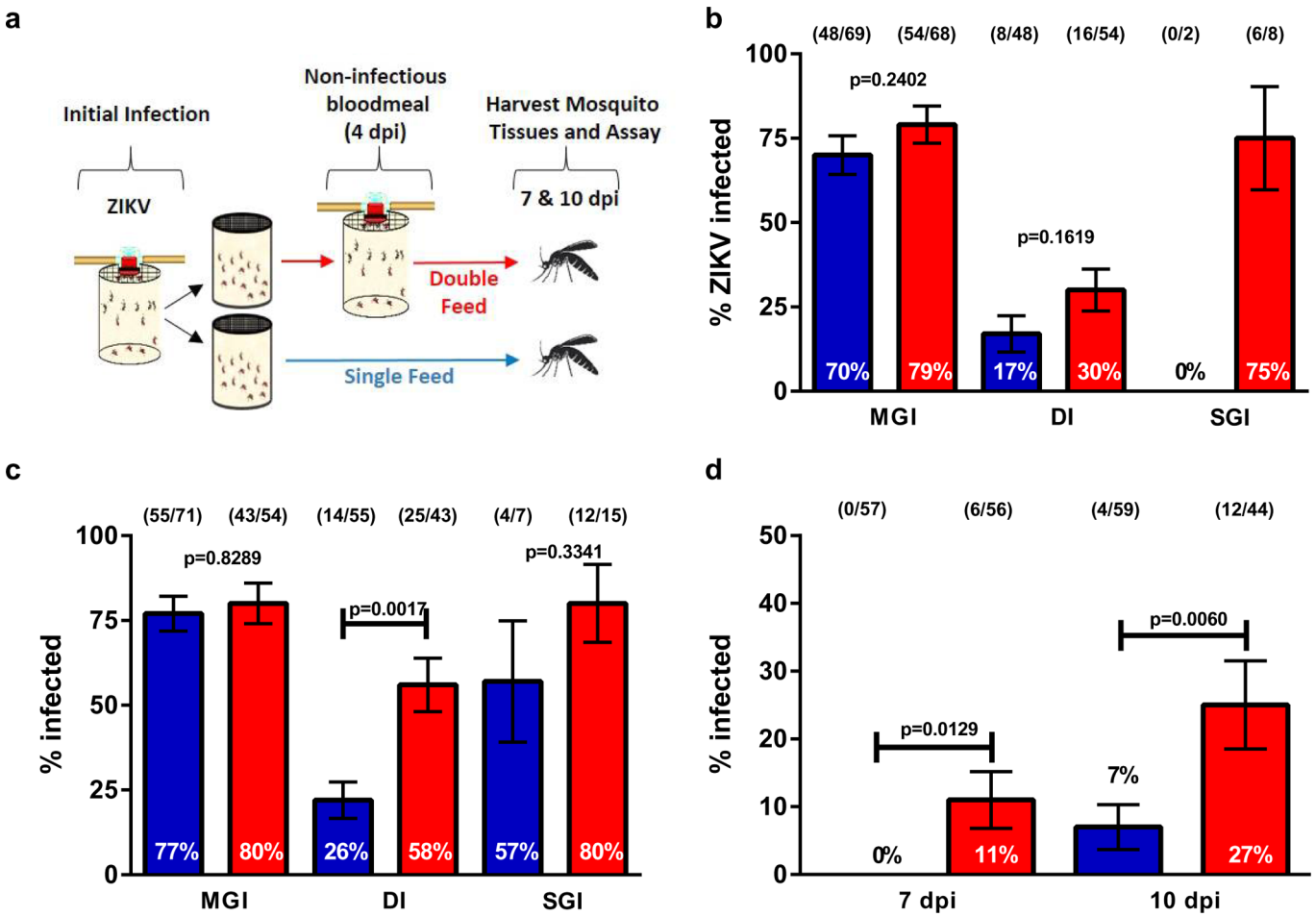


**Extended Data Fig. 3 | Multiple feeding events increase the potential of *Aedes albopictus* to transmit ZIKV.** (a) Schematic of experimental design. Paired bodies (MGI; midgut infection; % of mosquitoes with viral RNA in their bodies), legs (DI; disseminated infection; % of body positive mosquitoes with viral RNA in their legs) and salivary glands (SGI; salivary gland infection; % of leg positive mosquitoes with viral RNA in their salivary glands) were collected and assayed for the presence of viral RNA (b) 7 dpi and (c) 10 dpi. (d) SGI data from (b) and (c) analyzed as the % of ZIKV-exposed mosquitoes with a salivary gland infection. The data presented represents at least three experimental replicates. (●) single-feed; (●) double-feed. Data were analyzed by Two-sided Fisher's exact test. (*) $p<0.05$, (**) $p<0.01$, (***) $p<0.001$. Sample sizes (represented as a fraction of positive samples/ total samples) for each treatment/ timepoint are embedded in the figures above each experimental group. Center values represent the proportion and error bars represent the binomial SE of sample proportions.

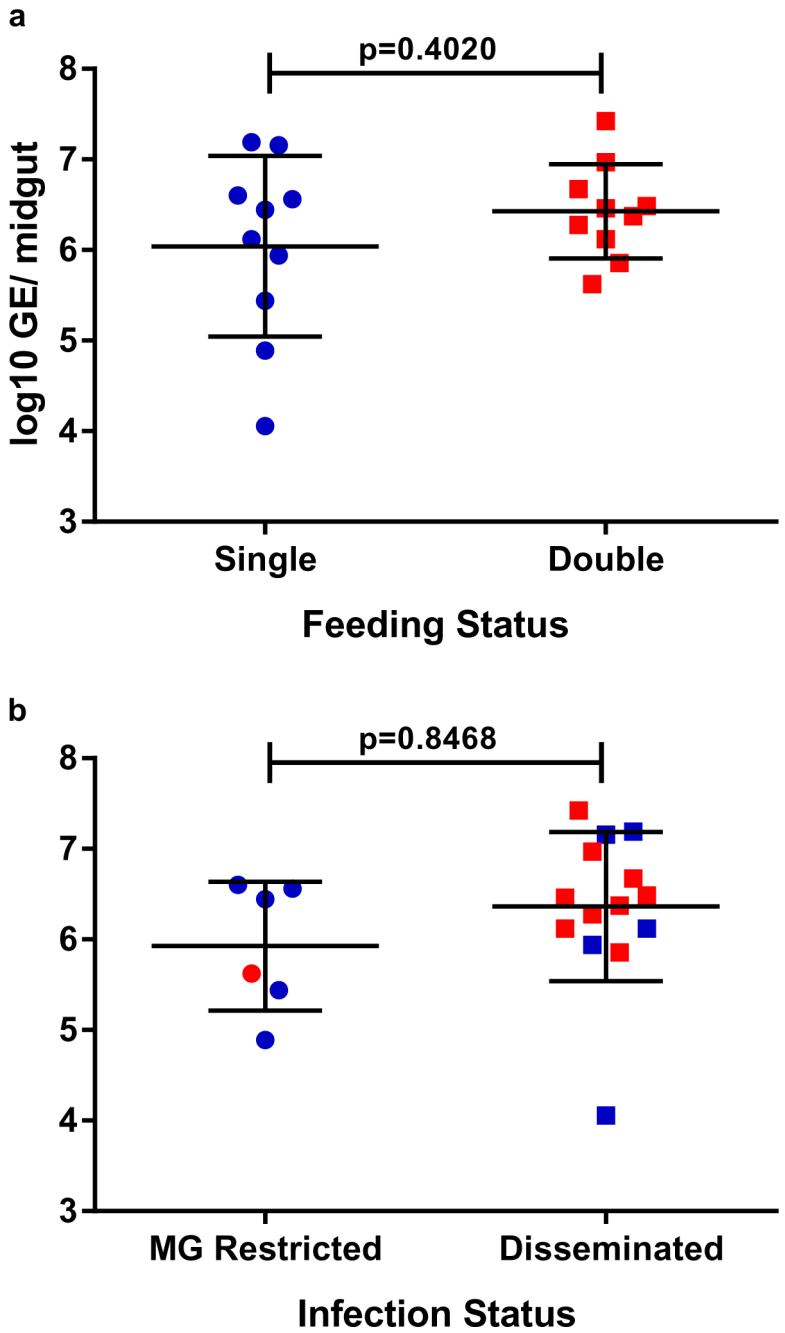


**Extended Data Fig. 4 | Increased dissemination rates associated with multiple feeding are not due to increased midgut replication.** *Aedes aegypti* mosquitoes were offered a ZIKV-infectious bloodmeal and 4 dpi individuals in the double feed groups were fed a second, non-infectious bloodmeal. At 7 dpi, mosquito midguts and legs were dissected and viral genomic equivalents were determined. (a) Midgut genome equivalents based on feeding status regardless if the infection was restricted to the midgut or disseminated (n=10/ group). (b) Midgut genome equivalents based on infection status (disseminated (n=14) vs. not disseminated (n=6) (that is midgut restricted)) regardless of feeding status. (●) single feed; (●) double feed. Data were analyzed by Two-sided T-test. Center values represent means and error bars represent SD.

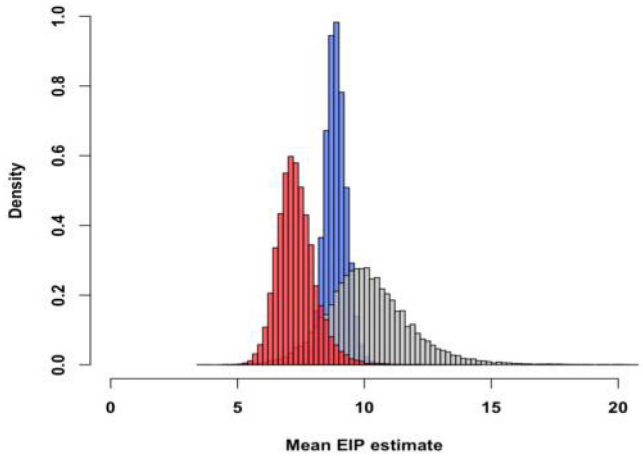


**Extended Data Fig. 5 | Distributions of mean EIP estimates.** (●) experimental single-feed; (●) meta-analysis single-feed; (●) double feed, from a thinned subset (10,000 iterations) of each model's respective posterior shape and rate estimates.

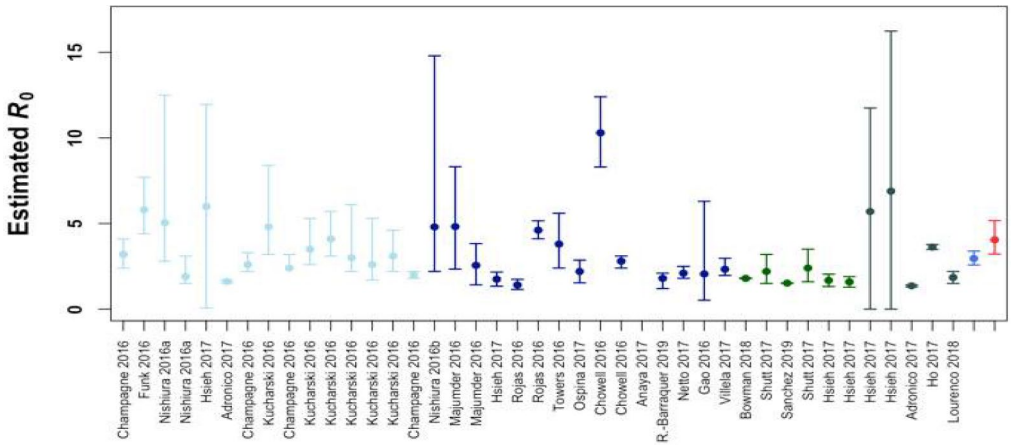


**Extended Data Fig. 6 | Comparison of $R_0$ estimates from experimental data to published estimates from field studies.** Circles correspond to point estimates of $R_0$ derived from an individual study and setting and/or methodology, while the lines show the corresponding 95% CI (n=41 estimates from 22 studies). Colors are used to show estimates from different regions (light blue: Oceania, dark blue: South America, dark green: Central America, gray: other) and our own experimental results (blue: single-feed model, red: double-feed model).

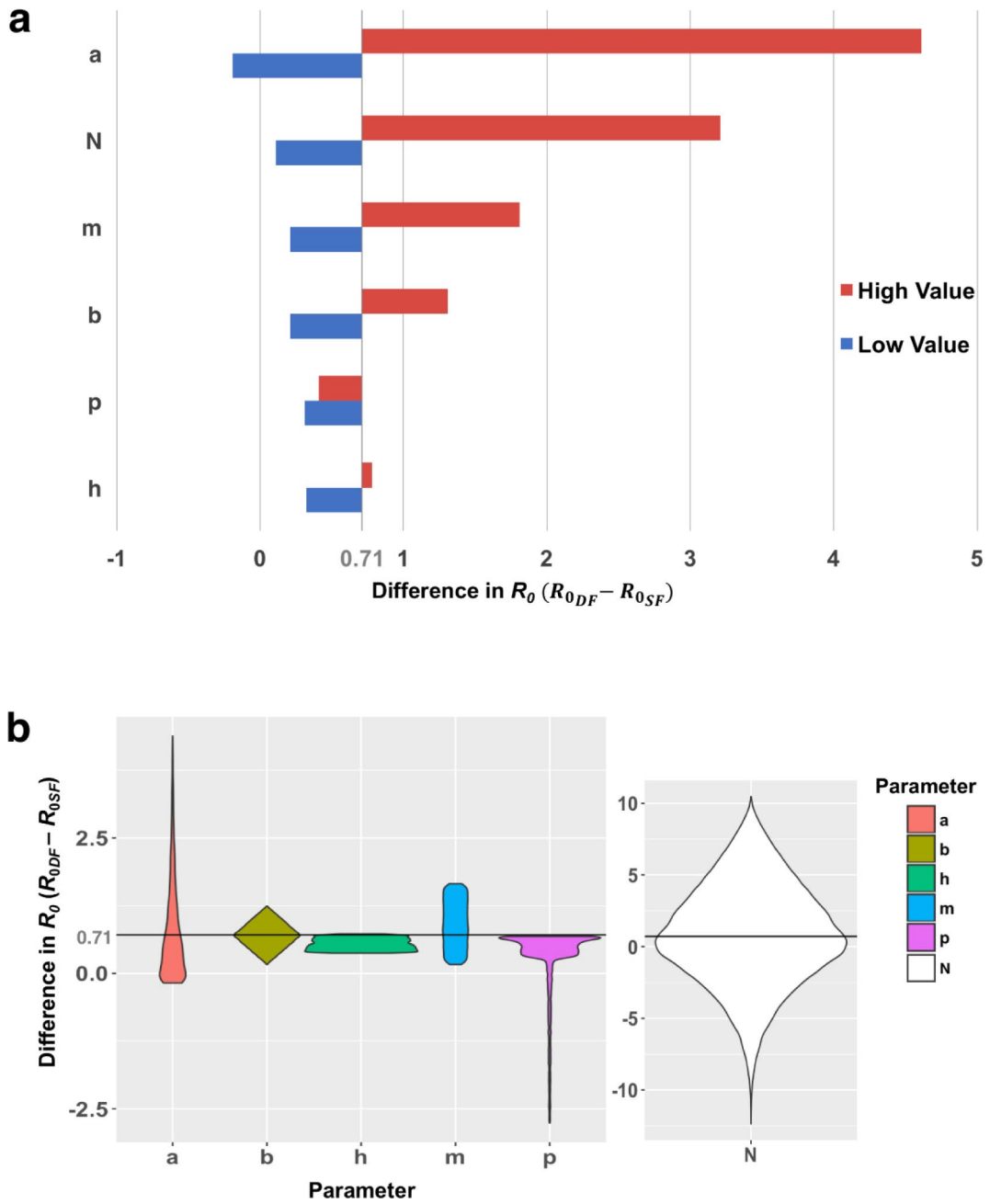


**Extended Data Fig. 7 | Results of a best/worst case scenario sensitivity analysis and a one-way random sampling sensitivity analysis.** (a) Scenario sensitivity analysis assessing the effect of varying each parameter according to its lowest and highest bounds on the difference in $R_0$ ($R_{0_{DF}} - R_{0_{SF}}$) (blue=lowest value; red=highest value for each parameter). The initial difference of 0.71 was obtained by holding all parameters constant at their mean or given value (Supplementary Table 4). (b) Violin plots show the probably density of the difference in $R_0$ ($R_{0_{DF}} - R_{0_{SF}}$) when we randomly sampled each parameter 10,000 times from its specified distribution (Supplementary Table 4), while holding all other parameters constant. Each violin spans the 98% quantile of the distribution of $R_0$ differences with the width proportional to the probability of observing a particular value of difference. The horizontal line at 0.71 represents the difference in $R_0$ when all parameters are held constant at their mean or given value.

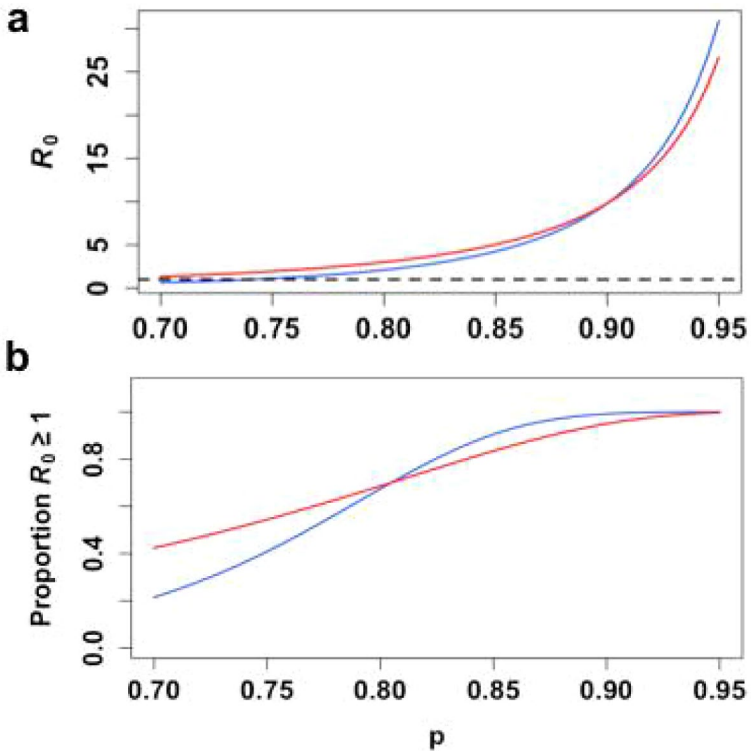


**Extended Data Fig. 8 | Comparison of $R_0$ and *p*.** (a) The mean value for 10,000 simulations of $R_0$ is plotted for every value of *p* (blue= single-feed model, red= double-feed model, dashed black= reference line at $R_0$=1), along with (b) the proportion of those simulations for which $R_0$ >1.

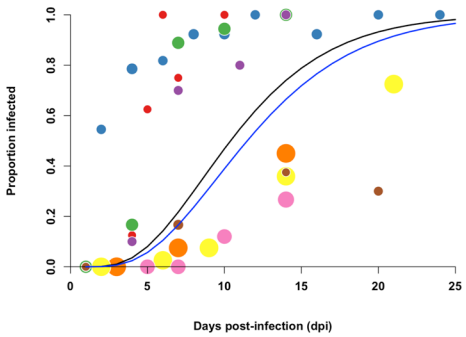


**Extended Data Fig. 9 | Salivary Gland Infection Meta-Analysis.** Salivary Gland Infection (SGI) data aggregated from 8 published studies are plotted, with each observation (n=45) weighted by sample size and color-coded by study. The black line shows the best-fit gamma CDF model for salivary gland data and the blue line for combined meta-analysis single-feed dissemination data (data points not shown).

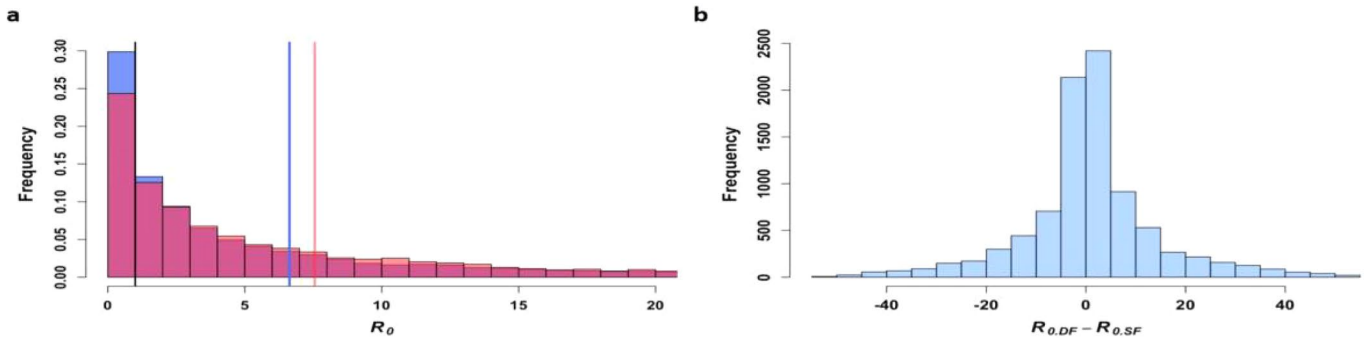


**Extended Data Fig. 10 | Results of an uncertainty analysis assessing the distribution of $R_0$ under different feeding assumptions.** (a) We compared histograms of the single-feed $R_0$ distribution specified by the uncertainty analysis (blue) and double-feed $R_0$ distribution (red) and the overlap (purple) generated from 10,000 iterations of Latin Hypercube Sampling. The mean $R_0$ for each respective distribution is also shown as a horizontal line ($R_{0_{SF}} = 6.68$ , $R_{0_{DF}} = 7.55$). (b) The distribution of the difference in $R_0$ ($R_{0_{DF}} - R_{0_{SF}}$) is plotted for each random sample (n=10,000).

nature research

Corresponding author(s): Doug E. Brackney & Philip M Armtrong

Last updated by author(s): October 16, 2019

# Reporting Summary

Nature Research wishes to improve the reproducibility of the work that we publish. This form provides structure for consistency and transparency in reporting. For further information on Nature Research policies, see Authors & Referees and the Editorial Policy Checklist.

## Statistics

For all statistical analyses, confirm that the following items are present in the figure legend, table legend, main text, or Methods section.

| n/a | Confirmed | |
|---|---|---|
| ☐ | ☒ | The exact sample size (*n*) for each experimental group/condition, given as a discrete number and unit of measurement |
| ☐ | ☒ | A statement on whether measurements were taken from distinct samples or whether the same sample was measured repeatedly |
| ☐ | ☒ | The statistical test(s) used AND whether they are one- or two-sided<br>*Only common tests should be described solely by name; describe more complex techniques in the Methods section.* |
| ☐ | ☒ | A description of all covariates tested |
| ☐ | ☒ | A description of any assumptions or corrections, such as tests of normality and adjustment for multiple comparisons |
| ☐ | ☒ | A full description of the statistical parameters including central tendency (e.g. means) or other basic estimates (e.g. regression coefficient) AND variation (e.g. standard deviation) or associated estimates of uncertainty (e.g. confidence intervals) |
| ☐ | ☒ | For null hypothesis testing, the test statistic (e.g. *F*, *t*, *r*) with confidence intervals, effect sizes, degrees of freedom and *P* value noted<br>*Give P values as exact values whenever suitable.* |
| ☐ | ☒ | For Bayesian analysis, information on the choice of priors and Markov chain Monte Carlo settings |
| ☒ | ☐ | For hierarchical and complex designs, identification of the appropriate level for tests and full reporting of outcomes |
| ☐ | ☒ | Estimates of effect sizes (e.g. Cohen's *d*, Pearson's *r*), indicating how they were calculated |

*Our web collection on statistics for biologists contains articles on many of the points above.*

## Software and code

Policy information about availability of computer code

| | |
|---|---|
| Data collection | Data was recorded and organized in Microsoft Excel 2010 (v 14.0). |
| Data analysis | Statistical analysis of experimental data was performed in GraphPad Prism 6. All modeling analyses were run using R software version 3.5.1. Posterior distributions of model parameters were estimated via a Markov chain Monte Carlo sampling algorithm implemented in JAGS version 4.3.0 using the rjags package. Latin Hypercube Sampling was performed with the randomLHS function of the lhs package. Model-related graphics were created using the ggplot2 and plotrix packages. |

For manuscripts utilizing custom algorithms or software that are central to the research but not yet described in published literature, software must be made available to editors/reviewers. We strongly encourage code deposition in a community repository (e.g. GitHub). See the Nature Research guidelines for submitting code & software for further information.

## Data

Policy information about availability of data

All manuscripts must include a data availability statement. This statement should provide the following information, where applicable:

- Accession codes, unique identifiers, or web links for publicly available datasets
- A list of figures that have associated raw data
- A description of any restrictions on data availability

Numerical source data underlying the graphs shown in figures 1 and 2c are associated with each figure. Additional data that support the findings of this study are available from the corresponding author upon request.

# Field-specific reporting

Please select the one below that is the best fit for your research. If you are not sure, read the appropriate sections before making your selection.

☒ Life sciences ☐ Behavioural & social sciences ☐ Ecological, evolutionary & environmental sciences

For a reference copy of the document with all sections, see nature.com/documents/nr-reporting-summary-flat.pdf

# Life sciences study design

All studies must disclose on these points even when the disclosure is negative.

| | |
|---|---|
| Sample size | Statistical methods were not used to predetermine sample size. Instead we followed the established precedence in the literature and in most of the experiments exceeded that precedence |
| Data exclusions | No data were excluded from the analysis. |
| Replication | The data were pooled from two to three independent replicates for each experiment involving mosquitoes. Although the magnitude of difference between the single- and double-feed groups varied for each experimental replicate, enhancement itself was observed in every replicate. All attempts were made to thoroughly describe the methods in this manuscript so as to provide a template for reproduction. |
| Randomization | Per experiment, all mosquitoes were from the same rearing cohort. The mosquitoes were randomly separated into two groups; either single feed or double feed groups. All environmental conditions were kept constant through the duration of the experiment. Litters of sucking mice were randomly assigned to cohorts of mosquitoes and individual suckling mice were randomly assigned to individual mosquitoes within the respective cohorts for the transmission studies . |
| Blinding | Mosquito samples were harvested by one group of researchers and processed and data analyzed by another. Similar to the mosquito samples, the right front leg of mice exposed to CHIKV infected mosquitoes were collected by one group and provided to a second group for processing and data analysis. Group 2 was unaware of the order in which samples were given to them. Only after processing and data analysis were completed for each experimental replicate were the treatments made aware to the sample order. |

# Reporting for specific materials, systems and methods

We require information from authors about some types of materials, experimental systems and methods used in many studies. Here, indicate whether each material, system or method listed is relevant to your study. If you are not sure if a list item applies to your research, read the appropriate section before selecting a response.

## Materials & experimental systems

| n/a | Involved in the study |
|---|---|
| ☐ | ☒ Antibodies |
| ☐ | ☒ Eukaryotic cell lines |
| ☒ | ☐ Palaeontology |
| ☐ | ☒ Animals and other organisms |
| ☒ | ☐ Human research participants |
| ☒ | ☐ Clinical data |

## Methods

| n/a | Involved in the study |
|---|---|
| ☒ | ☐ ChIP-seq |
| ☒ | ☐ Flow cytometry |
| ☒ | ☐ MRI-based neuroimaging |

## Antibodies

| | |
|---|---|
| Antibodies used | All antibodies used in this study are commercially available from Fisher Scientific-Invitrogen. Flavivirus envelope antibody (clone FE1) (Catalog#171258; Lot# QJ2092901) was used at a dilution of 1:200 for the detection of ZIKV antigen in the gut of mosquitoes. The secondary antibody used was an AlexaFluor488 goat anti-mouse IgG (H+L) (Catalog# A11001; Lot# 745480) at a dilution of 1:200. |
| Validation | Antibodies were validated by the manufacturer (Fisher Scientific-Invitrogen). |

## Eukaryotic cell lines

Policy information about cell lines

| | |
|---|---|
| Cell line source(s) | All mosquito and vertebrate cell lines used in these studies were acquired from ATCC. |
| Authentication | These cell lines were authenticated by ATCC, but have not been authenticated by us. |

| | |
|---|---|
| Mycoplasma contamination | The cell lines are routinely monitored for mycoplasma contamination and the cell lines used in this study tested negative for mycoplasma. |
| Commonly misidentified lines (See ICLAC register) | None of the cell lines used are commonly misidentified. |

## Animals and other organisms

Policy information about studies involving animals; ARRIVE guidelines recommended for reporting animal research

| | |
|---|---|
| Laboratory animals | Suckling mice used in this study were CD-1 strain, of mixed sex, approximately 5 days old and obtained from Charles River Laboratories (Wilmington, MA). Aedes aegypti (Orlando strain, collected from Orlando, FL in 1952 and Poza Rica strain, collected from Poza Rica Mexico in 2016) and Aedes albopictus (Stratford strain, generation F5, collected in Stratford, CT, 2015) were used in these studies. Only female mosquitoes approximately 7 days post emergence were used for all studies. |
| Wild animals | N/A |
| Field-collected samples | N/A |
| Ethics oversight | All experiments involving mice were approved by and preformed under the Animal Care and Use Committee at The Connecticut Agricultural Experiment Station (P28-17). |

Note that full information on the approval of the study protocol must also be provided in the manuscript.